

Ezh2 promotes clock function and hematopoiesis independent of histone methyltransferase activity in zebrafish

Yingbin Zhong^{1,2}, Qiang Ye^{1,2}, Chengyan Chen^{1,2}, Mingyong Wang^{1,2} and Han Wang^{1,2,*}

¹Center for Circadian Clocks, Soochow University, Suzhou, Jiangsu, PR China and ²School of Biology & Basic Medical Sciences, Medical College, Soochow University, Suzhou, Jiangsu, PR China

Received September 13, 2017; Revised January 30, 2018; Editorial Decision February 01, 2018; Accepted February 06, 2018

ABSTRACT

EZH2 is a subunit of polycomb repressive complex 2 (PRC2) that silences gene transcription via H3K27me3 and was shown to be essential for mammalian liver circadian regulation and hematopoiesis through gene silencing. Much less, however, is known about how Ezh2 acts in live zebrafish. Here, we show that zebrafish *ezh2* is regulated directly by the circadian clock via both E-box and RORE motif, while core circadian clock genes *per1a*, *per1b*, *cry1aa* and *cry1ab* are down-regulated in *ezh2* null mutant and *ezh2* morphant zebrafish, and either knockdown or overexpression of *ezh2* alters locomotor rhythms, indicating that Ezh2 is required for zebrafish circadian regulation. In contrast to its canonical silencing function, zebrafish Ezh2 up-regulates these key circadian clock genes independent of histone methyltransferase activity by directly binding to key circadian clock proteins. Similarly, Ezh2 contributes to hematopoiesis by enhancing expression of hematopoietic genes such as *cmyb* and *lck*. Together, our findings demonstrate for the first time that Ezh2 acts in both circadian regulation and hematopoiesis independent of silencing PRC2.

INTRODUCTION

Circadian rhythms are endogenous oscillations generated by interlocking negative transcriptional and translational feedback loops, allowing for organisms to coordinate physiological and behavioral rhythms with a period ~24 h for anticipating environmental changes (1). In mammals, molecular oscillators operate in the master clock, the suprachiasmatic nucleus (SCN) in the hypothalamus of the brain (2) and also in peripheral organs or tissues (3,4). The bHLH-PAS proteins CLOCK and BMAL1 form a heterodimer to drive transcription of *Period* genes (*Per1*, *Per2* and *Per3*) and *Cryptochrome* genes (*Cry1* and *Cry2*) through E-boxes

(5). PER and CRY proteins then are translocated into the nucleus, and interact with the CLOCK–BMAL1 complex to repress their own expression (6). CLOCK and BMAL1 also drive the expression of the orphan nuclear receptor *Rev-erba* in the SCN and liver (7). *Bmal1* contains Rev-Erb α /ROR response elements (ROREs) in its promoter, and its expression is activated by ROR α but repressed by Rev-Erb α (7).

Roles of histone modifiers in circadian regulation have recently been investigated (8). In mice, transcriptional activation of *Per1* and *Per2* correlates with rhythmic acetylation of histone H3 at their promoter regions (9,10). In addition to histone acetylation, histone methylation also has been suggested to be important for circadian regulation. WDR5, a member of a histone methyltransferase complex, mediates rhythmic methylation of H3K4 and H3K9 at the promoters of PER1-regulated genes (11), and methylation of H3K4 and H3K9 are in phase with transcriptional activity of *Dbp* (*albumin D-site binding protein*) (12). JMJD5 and JMJD30, two Jumonji C domain-containing histone demethylase proteins, function in both the plant and human circadian systems (13,14).

Polycomb group proteins (PcG) are involved in heritable epigenetic regulation of gene expression during development (15). To date, two principal polycomb repressive complexes (PRCs), PRC1 and PRC2, have been identified (16). Mammalian PRC1 contains CBX, MPH, RING, BMI1 and MEL185, whereas PRC2 contains EZH, EED and SU(Z)12 (16). EZH2, enhancer of zeste homolog 2, silences gene transcription through trimethylation of histone H3 lysine 27 (H3K27me3) via its SET domain (17) and is essential for early development and tumor progression in most model organisms (18–20). However, EZH2 also functions positively independent of PRC2 in various cancers (21–24). For instance, EZH2 oncogenic activity in castration-resistant prostate cancer cells is independent of H3K27me3 (24,25). Interestingly, EZH2 was shown to be required for the mouse liver clock through binding to the clock complex and mediating methylation of H3K27 at the promoters of *Per1* and *Per2* (26). BMAL1 inhibits tumorigenesis and increases

*To whom correspondence should be addressed. Tel: +86 512 65882115; Fax: +86 512 65882115; Email: han.wang88@gmail.com

paclitaxel sensitivity in tongue squamous cell carcinoma through interaction with EZH2 (27).

In addition to its involvement in circadian regulation, EZH2 also was shown to play important roles for normal and malignant hematopoiesis (28,29). EZH2 was shown to be critical for B-cell development (30), and overexpression of mutated *EZH2* was observed in B- and T-cell lymphoproliferative disorders and myeloid malignancy (28). During early megakaryopoiesis, Notch1 intracellular domain increases cytoplasmic EZH2 levels (31) and GATA-1 utilizes IKAROS and EZH2 to promote erythropoiesis through suppressing *HES1* (32). *EZH2* is up-regulated with differentiation of bone marrow cells (33) and down-regulated during differentiation of HL-60 cells to mature granulocytes (34). Ectopic expression of *Ezh2* in the hematopoietic system increases the repopulation potential of hematopoietic stem cells (HSCs) and serial transplantation of these *Ezh2*-overexpressing HSCs resulted in mice developing myeloproliferative neoplasm (35).

Because *Ezh2* knockout mice cease development at early gastrulation (19), circadian roles of EZH2 in live animals, and its functions during hematopoiesis are far from certain to date. Zebrafish have become an attractive vertebrate model organism for studying circadian rhythms (36–39) and hematopoiesis (40). Here, we found that zebrafish *ezh2* is regulated directly by the circadian clock. Loss of *Ezh2* disrupts rhythmic expression of circadian clock genes and either knockdown or overexpression of *ezh2* alters locomotor rhythms of zebrafish larvae. Loss of *Ezh2* also results in defects in zebrafish primitive and definitive hematopoiesis. In contrast to its predominant gene silencing, *Ezh2* enhances circadian regulation and hematopoiesis independent of silencing PRC2 in zebrafish.

MATERIALS AND METHODS

Experimental animals

Wild-type zebrafish (*Danio rerio*), *ezh2* heterozygous, *per1b*^{-/-} mutant (41), *rev-erba*^{-/-} mutant (42), *Tg(gatal:DsRED)* (43), *Tg(mpx:EGFP)* (44), *Tg(lyz:EGFP)* (45), *Tg(cmyb:EGFP)* (46) and *Tg(coro1a:EGFP)* (47) zebrafish lines were maintained on a 14-h light/10-h dark cycle and fed three times daily at the Soochow University Zebrafish Facility. Embryos were obtained by natural crosses and fertilized eggs were raised at 28.5°C. PTU (2-phenylthiourea) (0.003%, wt/vol) was added to embryo medium to inhibit pigment formation for whole mount *in situ* hybridization experiments. All experiments were conducted in accordance with guidelines approved by the Soochow University Committee on the Use and Care of Animals.

Plasmid construction

cDNAs of zebrafish *ezh2* and mice *Ezh2* were PCR amplified with primer pairs *ezh2*F3 and *ezh2*R3, *mEzh2*F and *mEzh2*R, and cloned into pCDNA3.1/Myc-His(-) with XhoI and BamHI sites, respectively. Zebrafish *eed* cDNA was PCR amplified with primers *eed*F and *eed*R, and cloned into pCDNA3.1/Myc-His(-) with XhoI and EcoRI sites. Zebrafish *ezh2* cDNA was PCR amplified with primer pair

*ezh2*F4 and *ezh2*R4 and cloned into pDNA3.1-HA with BamHI and XhoI sites. Two amino acids, Phe681 and His703, critical for zebrafish *Ezh2* H3K27 methyltransferase activity (25,48,49) were mutated to Ile and Ala to generate the mutated form of zebrafish *ezh2* by two rounds of mutagenesis using primer pairs *ezh2*F681F and *ezh2*F681R, *ezh2*H703AF and *ezh2*H703AR, respectively. Similarly, the mutated form of mouse *Ezh2* with mutations at F667I and H689A was generated with primer pairs *mEzh2*F667IF and *mEzh2*F667IR, *mEzh2*H689AF and *mEzh2*H689AR.

An *ezh2* RNA probe for whole mount *in situ* hybridization was prepared as described previously (50). The fragment containing *ezh2* E-box was amplified with primers *ezh2*-E-luc-F and *ezh2*-E-luc-R, while the fragment containing *ezh2* RORE was amplified with primers *ezh2*-R-luc-F and *ezh2*-R-luc-R, and then both fragments were inserted into the pGL3.17-promoter vector with *Sac*I and *Xho*I sites, respectively, generating *ezh2*-E-luc and *ezh2*-R-luc. Then, the E-box sequence, CACGTG, was mutated to CCCGTC, with primers *ezh2*-Emu-F and *ezh2*-Emu-R, and the RORE sequence, TTGGGTC, also was mutated to TTCCCTC, with primers *ezh2*-Rmu-F and *ezh2*-Rmu-R. The *cmyb* and *lck* promoter fragments containing E-boxes were amplified with primer pairs *cmyb*-E-luc-F and *cmyb*-E-luc-R, *lck*-E-luc-F and *lck*-E-luc-R, respectively, and then both fragments were inserted into the pGL3.17-promoter vector with KpnI and XhoI sites, respectively, generating *cmyb*-luc and *lck*-luc. Plasmids for *bmal1b*, *clock1a* and *cry1aa* were constructed elsewhere (41). All primers are listed in Supplementary Table S1.

Generation of *ezh2*^{-/-} mutant zebrafish

The ENU-induced *ezh2*^{-/-} mutant zebrafish (sal199) was recovered from the Zebrafish Mutation Project (51). A point mutation (C to T) results in a premature stop codon that leads to a truncated protein of only 17 amino acids (aa). The fragment containing the mutation was PCR amplified with primers *ezh2*F1 and *ezh2*R1 (Supplementary Table S1), and confirmed by DNA sequencing. *ezh2* homozygous zebrafish was obtained by incrossing *ezh2* heterozygotes.

Generation of *ezh2* heat shock-inducible transgenic zebrafish

Transgenic zebrafish were generated using the Tol2-basse Multisite Gateway system (52). Briefly, zebrafish *ezh2* or mutated *ezh2* was cloned into the pME-MCS vector with XhoI and BamHI sites, using primers *ezh2*pMEF and *ezh2*pMER (Supplementary Table S1). The resulting plasmids, pME-*ezh2* and pME-*ezh2m*, were mixed with p5E-*hsp70l*, p3E-polyA and pDestTol2CG2 (EGFP driven by the *cmlc2* promoter) and performed LR reaction, respectively, resulting in pDestTol2-*hsp70l:ezh2*;CG2 and pDestTol2-*hsp70l:ezh2m*;CG2. To generate transgenic fish, 50 pg of pDestTol2-*hsp70l:ezh2*;CG2 or pDestTol2-*hsp70l:ezh2m*;CG2 with 25 pg of Tol2 transposase mRNA was injected into one-cell stage zebrafish embryos, respectively. Then injected embryos were cultured in Petri dishes with embryo medium at 28.5°C for 3 days. The larvae with GFP fluorescence in the heart were selected and raised to adulthood. *Tg(hsp70l:ezh2;CG)* and

Tg(hsp70l:ezh2m;CG) were identified by EGFP fluorescence in the heart and confirmed by PCR using primers *ezh2-F5* and *ezh2-R5* (Supplementary Table S1). Transgenic larvae were heat shocked at 37°C for one hour at ZT0 or ZT12 and used for locomotor assays or qRT-PCR analyses.

Cell culture, transfection and luciferase assay

Human embryonic kidney (HEK) 293T cells purchased from American Type Culture Collection (Manassas, VA) were cultured according to ATCC's instructions. Transfection and luciferase assays were performed as described previously (53). Briefly, 0.05×10^6 HEK293T cells were seeded into 24-well plate. After growing to 90% confluency, cells were transfected with 50 ng of *per1b-luc* or other reporter vectors, 100 ng each of *bmallb* and *clock1a* with or without 600 ng of *ezh2*. pRL-TK was co-transfected to normalize transfection efficiency. Twenty four hours after transfection, cells were harvested to perform luciferase assays.

Co-immunoprecipitation and Western Blotting

HEK293T cells were seeded in 10-cm Petri dishes. After reaching 90% confluency, cells were transfected with 6 μ g each of *bmallb*-HA or *bmallb*-His, *clock1a*-Flag and *ezh2*-His or *ezh2*-HA, and 2 μ g of *cry1aa*-His. Forty eight hours after transfection, cells were lysed in RIPA buffer with protease inhibitor (Sigma) and subjected to co-immunoprecipitation (Co-IP) according to manufacturer's instructions (Sigma). Briefly, cell lysates were released with protein G-Sepharose beads conjugated with anti-HA antibodies. After washing five times, the precipitates were re-suspended in SDS-PAGE sample buffer, boiled for 5 min and run on 12% SDS-PAGE gel, and then western blotting (WB) was conducted with mouse monoclonal anti-His (Cell Signaling Technology), anti-HA (Sigma) or anti-Flag (Cell Signaling Technology) antibody or rabbit polyclonal anti-Tubulin antibody. To detect the protein levels in zebrafish embryos, 48-hpf wild-type and *ezh2*^{-/-} mutant embryos were collected and lysated with RIPA buffer, respectively. Equal amount of wild-type and *ezh2* embryo extracts were loaded on SDS-PAGE, and then WB was performed using antibodies against EZH2 (Millipore), Eed (Millipore), H3K27m3 (Millipore), H3K27m2 (Millipore), H3K27m1 (Millipore), H3 (Cell Signaling Technology).

Whole mount *in situ* hybridization (WISH) and quantitative real-time PCR analysis

Whole mount *in situ* hybridization (WISH) was conducted as previously described (54), zebrafish embryos were fixed with PFA at 26 hpf, 28 hpf or 96 hpf and the fixed embryos were dehydrated with methanol and stored at -20°C. Embryos were rehydrated with sequential rehydration solution and then incubated in 50% formamide hybridization buffer with DIG-labeled probes at 65°C for overnight. Nitro blue tetrazolium and 5-bromo-4-chloro-3-indolyl phosphate (Roche) were used for colorimetric detection. For each WISH experiment, 25–30 larvae were used. At least three independent WISH experiments were conducted for each probe.

For quantitative real-Time PCR (qRT-PCR) analysis, total RNAs were extracted using TRIzol Reagent (Invitrogen) according to the manufacturer's instruction. After DNase treatment, RNA (1 μ g) was reverse-transcribed with oligo(dT)₁₈ primers and M-MLV reverse transcriptase. qRT-PCR was carried out in an Step-One real-time PCR detection system (ABI) using SYBR[®] Premix Ex Taq[™] (Takara Bio Inc., Dalian, Liaoning). Primers for qRT-PCR are listed in Supplementary Table S2 and some were previously reported (41). At least three independent samples were examined each with triplicate for qRT-PCR. The mRNA level of interested genes were calculated using $2^{-\Delta\Delta C_T}$ method (55) and presented as relative (-fold) values of the control group after normalized by β -actin mRNA levels.

Chromatin immunoprecipitation (ChIP) assays

ChIP assays were performed as described previously (41). Briefly, two groups of 200 wild-type larvae at 120 or 132 hpf were collected, cross-linked in 2% formaldehyde at room temperature for 30 min, and the crosslinking was terminated by adding 1/10 V of 1.12 M glycine, followed by PBS washing (3 times, each for 10 min). The following procedures were performed according to the manufacturer's protocol (Millipore's ChIP assay kit). The purified rabbit or mouse IgG (Invitrogen) was used as negative controls. ChIP PCR reactions were performed using primers flanking the E-box, D-box, and RORE sites as well as primers not flanking the these sites in the 5' promoter regions of genes as controls, respectively. Primers for the ChIP-qPCR are listed in Supplementary Table S1.

Morpholino and mRNA microinjection

ezh2 translation blocking Morpholinos (*ezh2*-MO: 5'-CCG ATTTCTCCCGGTCAATCCCAT-3') and a standard control MO (cMO: 5'-CCTCTTACCTCAGTTACAATTATA-3') (Gene Tools) were re-suspended in water as a 4 mM stock solution and diluted to the appropriate concentrations for microinjections in 0.2% PhenolRed and 0.1 M KCl. Different amounts of *ezh2*-MO and control MO were injected into zebrafish embryos at one-two cell stage. The efficacy of *ezh2*-MO was determined by GFP reporter assays (56).

ezh2 mRNA was synthesized using a commercial kit and linearized plasmid DNA as a template (mMESSAGE mMACHINE kit; Ambion). 1 nl (200 pg) *ezh2* mRNA was microinjected into one-cell stage zebrafish embryos. After microinjection, embryos were raised in Petri dishes with embryo medium at 28.5°C. Embryos were collected for RNA extraction or fixed with PFA for *in situ* hybridization at 26 hpf and 28 hpf, respectively, and kept in methanol at -20°C until use.

Zebrafish behavioral assays

Zebrafish larvae behavioral assays were performed under both DD and LD conditions, respectively, as previously reported (41). Briefly, a single zebrafish larva was placed in each wells of 48-well plate at 4 dpf (24 wild-type, 24

ezh2 MO-injected or *ezh2*-overexpressing transgenic fish). For *ezh2*-overexpressing transgenic fish, the fish was heat shocked at 37°C for one hour at ZT12. The 48-well plate was placed inside the Zebrafish (Videotrack; ViewPoint Life Sciences, Montreal, France) where continuous infrared light and white light were illuminated from 9:00 A.M. to 11:00 P.M. (LD) and constant 10% dim light (30 lx) was illuminated throughout the procedure (DD) (57). Instruments were placed in a chamber to maintain a constant temperature of 28.5°C. The Videotrack quantization parameters were set as described previously (58). Locomotor activities of larvae were monitored for five consecutive days using an automated video-tracking system (ViewPoint Life Sciences), and the movement of each larva was recorded using Zebralab3.10 software (ViewPoint Life Sciences).

Deep sequencing-based transcriptome analysis

Total RNAs from *ezh2*^{-/-} mutant and wild-type zebrafish at 28 hpf were extracted and purified. A total amount of 3 µg RNA per sample was used for the RNA sample preparations. Sequencing libraries were generated using NEBNext® Ultra™ RNA Library Prep Kit (NEB, USA) following the manufacturer's instructions. Clustering of the index-coded samples was performed on a cBot Cluster Generation System using TruSeq PE Cluster Kit (Illumina, PE-401–3001). After clustering, the library preparations were sequenced on an Illumina HiSeq 2500 platform. Perl scripts were used for removing the adapter and duplication sequences, calculating the Q20, Q30, GC-content, and then generating the raw reads. Transcriptome assembly was performed according to the protocol described previously (59). Assembled sequences were batch blasted against the latest version of the annotated zebrafish genome assembly (GRCz10) and to determine their gene names and Ensembl IDs. Gene expression levels were estimated using FPKM values (fragments per kilobase of exon per million fragments mapped) by the Cufflinks software (60). Gene abundance differences between those samples were calculated based on the ratio of the FPKM values. For the Gene Ontology (GO) enrichment analysis, the differentially expressed genes (DEGs) was implemented by the Goseq R packages based Wallonia noncentral hyper-geometric distribution (61). For the Kyoto Encyclopedia of Genes and Genomes (KEGG) analysis, we used KOBAS software to test the statistical enrichment of DEGs in KEGG pathways to predict and classify functions of the DEGs (62).

Statistical analysis

Values are presented as means ± standard deviation (S.D.). Expression levels of genes were analyzed by the JTK cycle method (63), where $P < 0.05$ was considered as rhythmic expression. Differences between two groups were analyzed by unpaired Student's *t*-test and statistical significance was accepted at $P < 0.05$ or smaller.

RESULTS

Zebrafish *ezh2* is a circadian clock-controlled gene

While *Ezh2* is known to be regulated by various oncogenic transcription factors, miRNAs and non-coding RNAs

(18,64,65), little is known about its circadian regulation. We first examined expression of *ezh2* mRNA in two consecutive days with qRT-PCR. Results show that zebrafish *ezh2* mRNA is rhythmically expressed under both DD (Figure 1A) and LD conditions (Figure 1B). Because *Per1b* inhibits clock gene expression through E-box (41), and *Rev-erba* suppresses gene expression through RORE (42), we examined *ezh2* expression in *per1b*^{-/-} and *rev-erba*^{-/-} mutant zebrafish. Results show that *ezh2* mRNA is up-regulated in the *per1b*^{-/-} mutant (Figure 1C and D) and *rev-erba*^{-/-} mutant zebrafish (Figure 1E and F) under both DD (Figure 1C and E) and LD conditions (Figure 1E and F). These results suggest that zebrafish *ezh2* is controlled by the circadian clock.

Bioinformatic analysis revealed one E-box in the zebrafish *ezh2* promoter and one RORE in its first intron (Figure 1G), implying that zebrafish *ezh2* expression may be mediated by these *cis-regulatory* elements. We isolated the DNA fragments harboring the E-box and the RORE and cloned them into the pGL3.17-promoter vector, respectively. Luciferase reporter assays show that *ezh2* E-box-mediated luciferase activities are activated by the Clock1a-Bmal1b complex (Figure 1H) but repressed by *Cry1aa*, a negative element in the circadian clock; and these E-box-mediated luciferase activities were completely abolished when the E-box sequence, CACGTG, was mutated into CCCGTC (Figure 1H). Further, *ezh2* RORE-mediated luciferase activities are activated by *Rorα* but suppressed by *Rev-erba*, and these activities were diminished when RORE was mutated (Figure 1I). We also performed ChIP-qPCR assays with zebrafish embryos. Results show that *Bmal1b* rhythmically binds to the E-box in the *ezh2* promoter (Figure 1J and Supplemental Figure S1A), while *Rorα* rhythmically binds to the RORE in its first intron (Figure 1K and Supplemental Figure S1B). Together, these results indicate that zebrafish *ezh2* is regulated directly by the circadian clock via both E-box and RORE.

Generation and characterization of an *ezh2* null mutant zebrafish

To investigate the functions of *ezh2* *in vivo*, we recovered an ENU-induced *ezh2* mutant line (sa1199) from the Zebrafish Mutation Project (ZMP) (51). A point mutation (C to T) (Figure 2A) in Exon 2 (Figure 2B) results in a premature stop codon that leads to a truncated peptide with only 17 amino acids (aa), missing its major functional domains (Figure 2C). The *ezh2* heterozygous fish appear normal outwardly and can survive until adulthood, while *ezh2* homozygous embryos display a little curved tail and thin yolk sac extension ~28 hpf (hours postfertilization) (Figure 2D), short body length and small eyes after 48 hpf (Figure 2D), and die after 7 dpf (days postfertilization). We further confirmed this phenotype by knocking it down with an *ezh2* Morpholino (*ezh2*-MO). We conducted EGFP reporter assays to determine the efficacy of the *ezh2*-MO. As shown in Supplemental Figure S2, 4 ng *ezh2*-MO effectively inhibits *ezh2* expression. Results showed that *ezh2* morphants phenocopy the *ezh2*^{-/-} mutant (Supplemental Figure S3A and B).

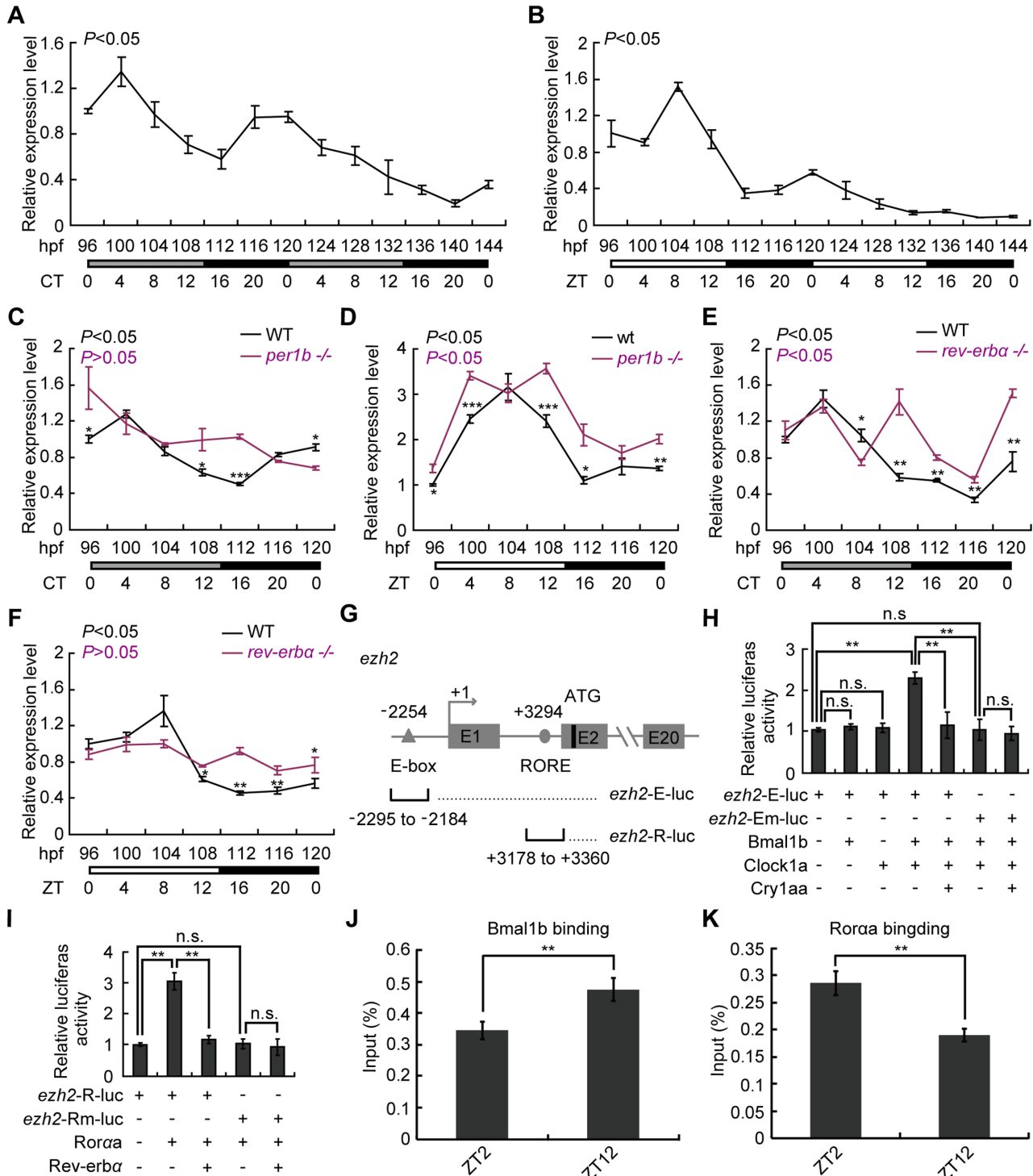


Figure 1. Zebrafish *ezh2* is a circadian clock-controlled gene. (A, B) *ezh2* is expressed rhythmically in developing zebrafish embryos under DD (A) and LD (B) conditions. (C–F) Up-regulation of *ezh2* in *per1b*^{-/-} (C, D) and *rev-erba*^{-/-} (E, F) mutant zebrafish under DD (C, E) and LD (D, F) conditions. For (A) to (F), at least three independent experiments were performed. Levels of mRNA expression were analyzed with the JTK-CYCLE method. ADJ.P for adjusted minimal *P*-values (*P* < 0.05). Student’s *t*-test was conducted. **P* < 0.05; ***P* < 0.01; ****P* < 0.001. (G) Schematic of the E-box in the *ezh2* promoter and the RORE in its first intron. The fragments containing the E-box and RORE were cloned into the pGL3.17-promoter vector, generating the *ezh2*-E-luc and *ezh2*-R-luc constructs, respectively. (H, I) Luciferase reporter assays show that *ezh2*-E-luc is activated by *Clock1a* and *Bmal1b* but inhibited by *Cry1aa* (H) and *ezh2*-R-luc is activated by *Roraα* but inhibited by *Rev-erba* (I). *ezh2*-Em-luc wherein the E-box was mutated; *ezh2*-Rm-luc wherein the RORE was mutated. Student’s *t*-test was performed. ***P* < 0.01. (J, K) ChIP-qPCR assays show that *Bmal1b* binds to the E-box region in the *ezh2* promoter (J) and *Roraα* binds to the RORE in the first intron (K). Student’s *t*-test was performed. ***P* < 0.01.

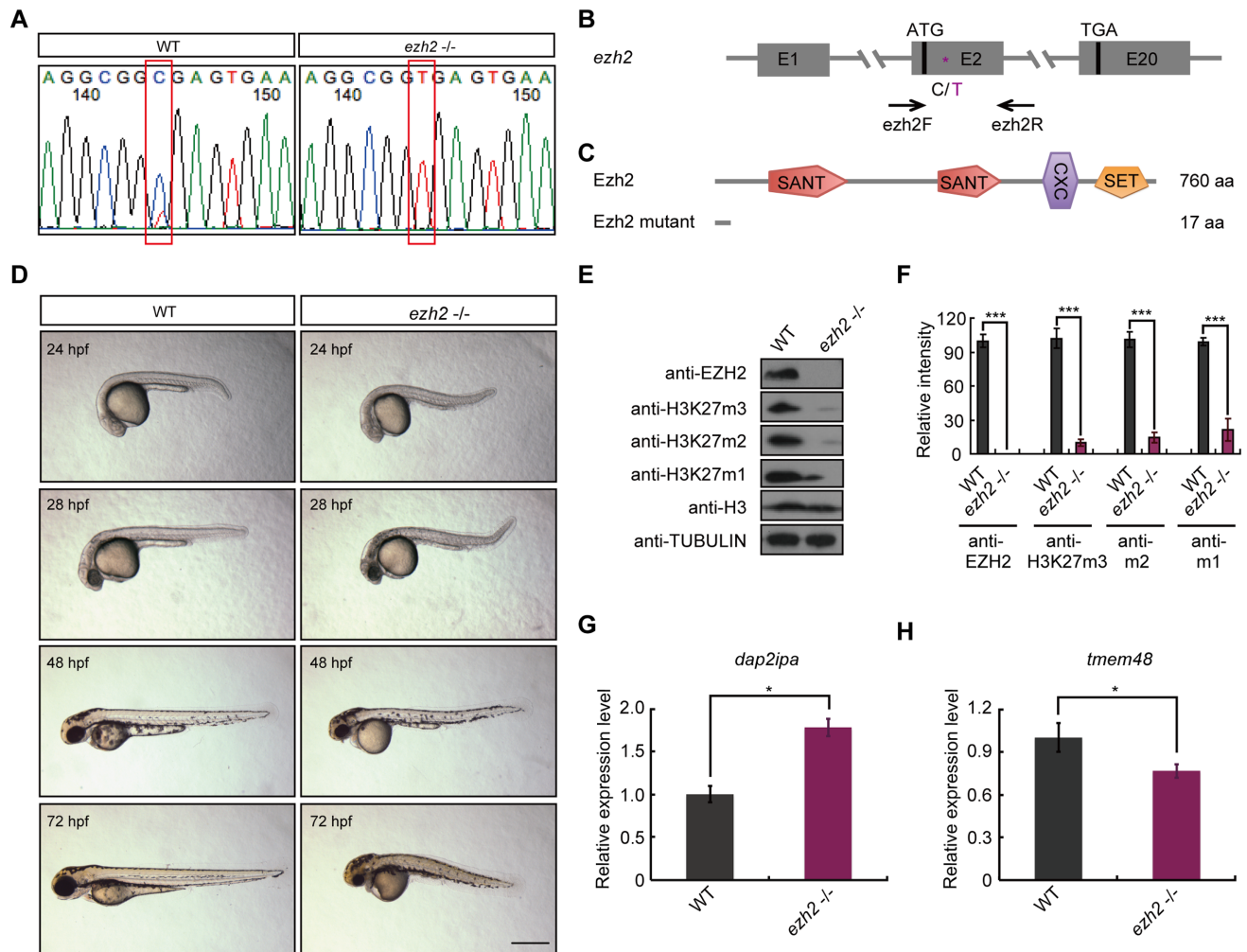


Figure 2. Generation and characterization of a zebrafish *ezh2* null mutant. (A) The C to T point mutation in the *ezh2* coding region was confirmed by DNA sequencing. WT, wild-type. (B) Gene structure of *ezh2* and the point mutation occurs in Exon 2. (C) The C to T nonsense mutation results in a truncated peptide and losses of its major functional domains. SANT, SWI3, ADA2, N-CoR and TFIIIB DNA-binding domains; CXC, Tesmin/TSO1-like CXC domain; SET, Su(var)3-9, Enhancer-of-zeste, Trithorax domain. (D) Images of WT and *ezh2*^{-/-} mutant zebrafish from 24 hpf to 72 hpf. Note that the *ezh2*^{-/-} mutant zebrafish display curved tail and thin yolk sac extension around 28 hpf and short body length and small eyes after 48 hpf. Scale bar, 0.5 mm. (E) Western Blotting shows that expression of Ezh2 is abolished and that of H3K27 mono-, di- and trimethylation are reduced in *ezh2*^{-/-} mutant fish. Proteins of zebrafish larvae were extracted with RIPA buffer at 48 hpf. Western Blotting was performed with indicated antibodies. (F) Quantification of western blotting images shown in (E) with ImageJ. Student's *t*-test was conducted. ****P* < 0.001. (G, H) qRT-PCR analysis of Ezh2-targeted gene *dab2ipa* (G) and *tmem48* (H) in 28 hpf WT and *ezh2*^{-/-} mutant zebrafish. Three independent experiments were conducted. Statistical analysis was performed using student's *t*-test. **P* < 0.05.

To examine whether this *ezh2* mutation is a null allele, we first performed western blotting analysis. Results show that the expression of Ezh2 protein is completely abolished, and mono-, di- and trimethylation of H3K27 are largely reduced in the mutant fish (Figure 2E and F), indicating that Ezh2 plays critical roles in regulating all methylations of H3K27 in zebrafish, which was reconfirmed with *ezh2* morphant embryos at 48 hpf (Supplemental Figure S3C). It has been reported that *DAB2IP* (DOC-2/DAB2 interactive protein) is repressed by EZH2 (66), while *tmem48* (NDC1 transmembrane nucleoporin) is activated by EZH2 (25). We examined expression of *dab2ipa* and *tmem48* in *ezh2*^{-/-} mutant zebrafish with qRT-PCR. Results show that *dab2ipa* is up-regulated (Figure 2G), while *tmem48* is down-regulated (Figure 2H) in *ezh2*^{-/-} mutant zebrafish, consistent with

previous results (25,66). These results suggest that the *ezh2*^{-/-} mutant zebrafish is a null allele.

Ezh2 plays important roles in the zebrafish circadian clock

EZH2 is shown to play an important role in the mouse liver circadian clock *in vitro* (26). To investigate the role of Ezh2 in zebrafish circadian regulation, we examined expression of core circadian clock genes in *ezh2*^{-/-} mutant fish by qRT-PCR. Results show down-regulation of *per1a*, *per1b*, *cry1aa*, and *cry1ab* in the *ezh2*^{-/-} mutant zebrafish under both DD and LD conditions (Figure 3A–H and Supplemental Figure S4A–H). Down-regulation of these genes is largely resulted from loss of *ezh2*, rather than zebrafish embryonic lethality, because we also observed that a zebrafish developmental gene, *her9* (67,68) and its target gene

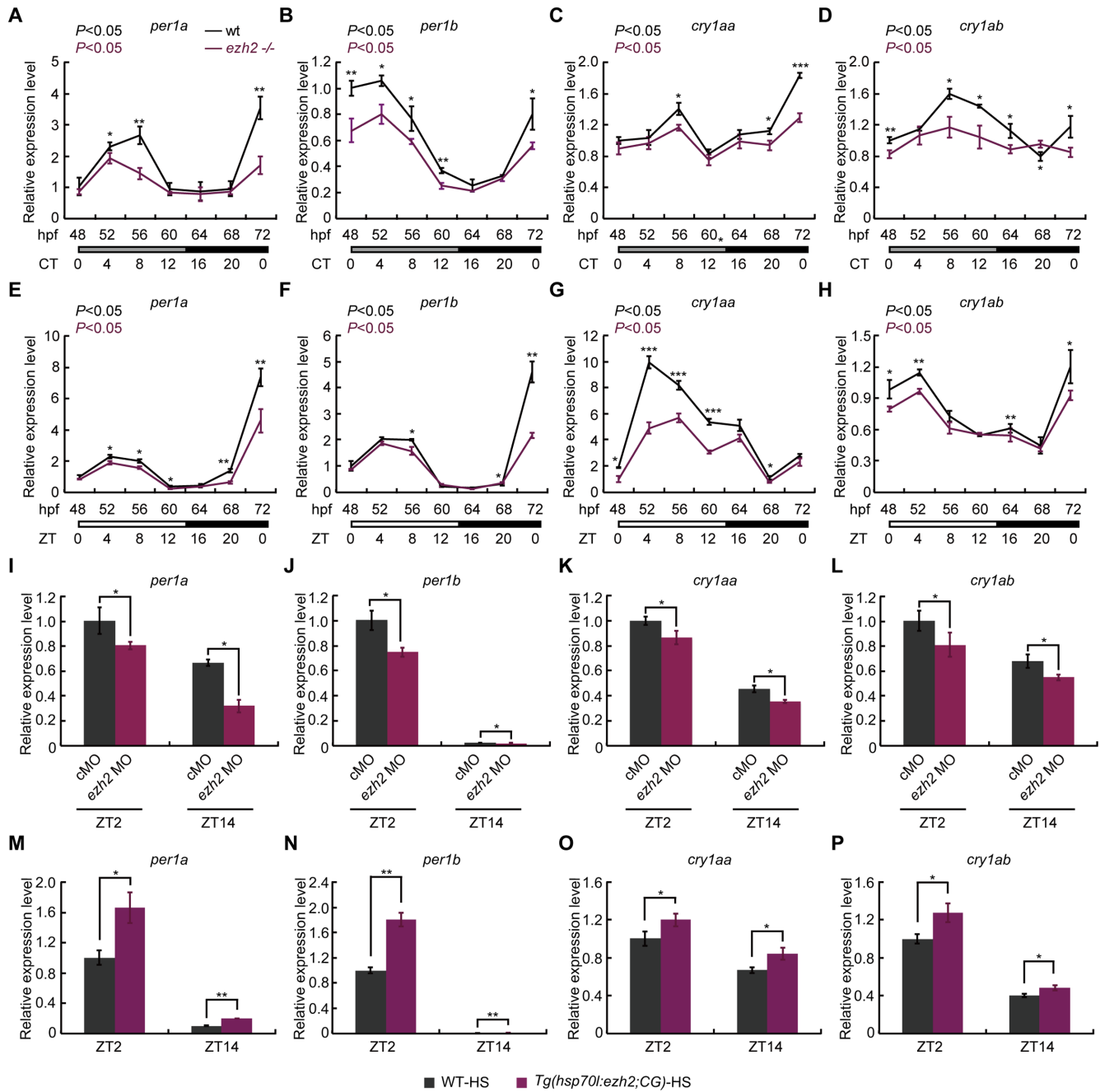


Figure 3. *Ezh2* is required for the zebrafish circadian clock. (A–H) qRT-PCR shows down-regulation of key circadian clock genes *per1a* (A, E), *per1b* (B, F), *cry1aa* (C, G), and *cry1ab* (D, H) in *ezh2*^{-/-} mutants under DD (A–D) and LD (E–H) conditions. Three independent experiments were conducted. mRNA expression levels were analyzed as in Figure 1. * $P < 0.05$; ** $P < 0.01$; *** $P < 0.001$. (I–L) Down-regulation of *per1a* (I), *per1b* (J), *cry1aa* (K) and *cry1ab* (L) in *ezh2* morphants. After injection, total RNAs were extracted at 26 hpf (ZT2) and 38 hpf (ZT14), respectively. Student's *t*-test was conducted. * $P < 0.05$. (M–P) Overexpression of *ezh2* driven by a heat shock promoter results in up-regulation of *per1a* (M), *per1b* (N), *cry1aa* (O) and *cry1ab* (P). Heat shock was conducted at ZT0 (96 hpf) and ZT12 (108 hpf) for 1 h, respectively, and samples were collected at ZT2 and ZT14. Three independent experiments were performed. Statistical analysis was performed using Student's *t*-test. * $P < 0.05$; ** $P < 0.01$.

dab2ipa are up-regulated (Figure 2G and Supplementary Figure S5) during early development. Moreover, knocking down *ezh2* by a Morpholino resulted in down-regulation of these circadian clock genes (Figure 3I–L). We then generated an *ezh2* heat shock-inducible transgenic zebrafish, *Tg(hsp70l:ezh2;CG2)* (Supplemental Figure S6). In contrast, qRT-PCR results showed that overexpression of *ezh2*

by either heat shock-induction or capped mRNA microinjection up-regulates these clock genes (Figure 3M–P and Supplemental Figure S7). These results suggest that *Ezh2* contributes to zebrafish circadian regulation.

The *ezh2*^{-/-} mutant zebrafish lose movement after 3 dpf. In order to examine the effects of *Ezh2* on zebrafish circadian regulation, we used *ezh2* morphants and

Tg(hsp70l:ezh2;CG2) fish to perform locomotor activity assays. Results showed that *ezh2* morphants display 0.2-h lengthened period (Figure 4A and B), reduced locomotor amplitude (Figure 4A and C) and 0.25-h delayed phase (Figure 4A and D) under DD condition, and enhanced locomotion activity under LD condition (Figure 4E–H); whereas overexpression of *ezh2* by heat shocking inducible promoter *hsp70l* led to 0.8-h shortened period (Figure 4I and J), elevated amplitude (Figure 4G and K) and 1.4-h advanced phase (Figure 4I and L) under DD condition, and elevated locomotor activities under LD condition (Figure 4M–P). It is intriguing that both the morphant larvae and heat shock-induced overexpressing larvae display elevated locomotor activities under LD condition, but the underlying mechanisms need further investigation. Together, these results indicate that Ezh2 plays important roles in the zebrafish circadian clock.

Zebrafish Ezh2 enhances clock gene expression independent of its histone methyltransferase activity

To delineate how zebrafish Ezh2 regulates the circadian clock, we performed Co-IP assays to examine whether zebrafish Ezh2 can interact with clock proteins. Results show that zebrafish Ezh2 binds to the Clock1a–Bmal1b–Cry1aa complex (Figure 5A and B). We also performed luciferase reporter assays with E-boxes-containing *per1b-luc*. Results show that *per1b* promoter activities are activated by the Clock1a–Bmal1b complex, and Ezh2 enhances Clock1a–Bmal1b-mediated activities in a dosage-dependent manner, while Cry1aa represses the activities (Figure 5C). However, EZH2 was shown to bind to the clock complex in the mouse liver, and particularly to enhance transcriptional repression mediated by mouse CRY proteins (26). Indeed, we reconfirmed the results that mouse EZH2 inhibits CLOCK–BMAL1 transcriptional activities on *Per1-luc* (Supplementary Figure S8A), implicating different mechanisms underlying roles of EZH2/Ezh2 in mice and zebrafish circadian regulation.

While EZH2 was shown to primarily mediate gene silencing via recruitment of the PRC2 (17), EZH2 also functions to enhance target genes in human cancers independent of PRC2 (24,25). We hypothesized that mouse EZH2 and zebrafish Ezh2 contribute to circadian regulation with different mechanisms. To examine this hypothesis, the two amino acid residuals, F681 and H703 in zebrafish and F667 and H689 in mice, critical for the Ezh2/EZH2 H3H27 methyltransferase activity were mutated (Supplementary Figure S9) (25,48,49), respectively. Luciferase reporter assays showed that zebrafish Ezh2 enhances Clock1a–Bmal1b transcriptional activity regardless of mutations of the two critical residuals (Figure 5D), and one of the PRC2 members, Eed, has no such activity (Figure 5D). Intriguingly, mouse EZH2 represses CLOCK–BMAL transcriptional activity (Supplementary Figure S8A). However, the mutated EZH2 loses this repressive activity and surprisingly elevates CLOCK–BMAL transcriptional activity (Supplementary Figure S8B). Moreover, Co-IP assays showed that Eed binds to Ezh2 but not Clock1a and Bmal1b in zebrafish (Figure 5E), suggesting that just Ezh2 alone, rather than PRC2, interacts with clock proteins. These results indicate

that Ezh2 enhances Bmal1b–Clock1a transcription activity independent of its histone methyltransferase activity in zebrafish.

We also examine the functions of Ezh2 *in vivo* by injecting *per1b-luc* and *ezh2* mRNA into wild-type or *ezh2*^{–/–} mutant zebrafish. Results showed that overexpressing *ezh2* up-regulates *per1b-luc* promoter activities in zebrafish embryos (Figure 5F), while *per1b-luc* activities are down-regulated in the *ezh2*^{–/–} mutant zebrafish embryos (Figure 5G). In line with *in vitro* result, *in vivo* Co-IP assays showed that Bmal1b binds to Ezh2 but not to Eed in zebrafish embryos (Figure 5H). ChIP-qPCR assays showed that both Bmal1b and Ezh2 rhythmically bind to the E-box in the *per1b* promoter (Figure 5I, J and Supplementary Figure S1C) and these bindings are largely reduced in *ezh2*^{–/–} mutant (Figure 5I and J). Moreover, zebrafish larvae overexpressing *ezh2* with two mutated residues by heat shock display 0.5-h shortened period, elevated amplitude and 0.8-h advanced phase of locomotor activities under DD condition (Supplementary Figure S10A–D), elevated locomotor activities under LD condition (Supplementary Figure S10E–H), and up-regulates *per1a*, *per1b*, *cry1aa* and *cry1ab* (Supplementary Figure S10I–L), similar to the results obtained from heat shock induction of wild-type Ezh2, further indicating that Ezh2 functions in zebrafish circadian regulation independent of PRC2.

Taken together, these results suggest that Ezh2 plays positive roles in circadian regulation by directly binding to key circadian clock proteins occupying the E-box containing promoter region, and Ezh2 enhances clock function independent of its histone methyltransferase activity.

Hematopoietic defects in *ezh2*^{–/–} mutant zebrafish

EZH2 is known to play important roles in normal and malignant hematopoiesis *in vitro* (16,29). However, the *in vivo* role of Ezh2 in hematopoiesis is still unclear. Whole mount *in situ* hybridization (WISH) shows that *ezh2* is expressed in the ICM (intermediate cell mass) at 24, 28 and 33 hpf and PBI (posterior blood island) at 33 hpf (Supplementary Figure S11), consistent with a previous observation (50). We also observed that *ezh2*^{–/–} mutant embryos display reduced blood cells at 32 hpf (Supplemental Movie S1). To search for Ezh2-affected genes involved in hematopoiesis, we performed high-throughput RNA sequencing of *ezh2*^{–/–} mutant and wild-type embryos at 28 hpf. The transcriptome analysis reveals 893 up-regulated genes and 425 down-regulated genes in the *ezh2*^{–/–} mutant zebrafish (Figure 6A, and Supplementary Table S2) (The data was deposited into NCBI Gene Expression Omnibus, GEO accession number GSE103913). Further, both GO (Gene Ontology) and KEGG (Kyoto Encyclopedia of Genes and Genomes) analyses of these DEGs show that genes involved in developmental processes, transcriptional activities, MAPK and calcium signaling pathways, and vascular smooth muscle contraction are markedly altered in the *ezh2*^{–/–} mutant (Supplemental Figure S12). In particular, genes related to hematopoiesis, such as *hbaa1*, *cmyb*, *gata1a*, *scl*, *alas2*, *hbbe1*, *hbbe3*, *hbbe3*, *hbae3* and *hbae1*, are down-regulated (Figure 6B), which was reconfirmed with

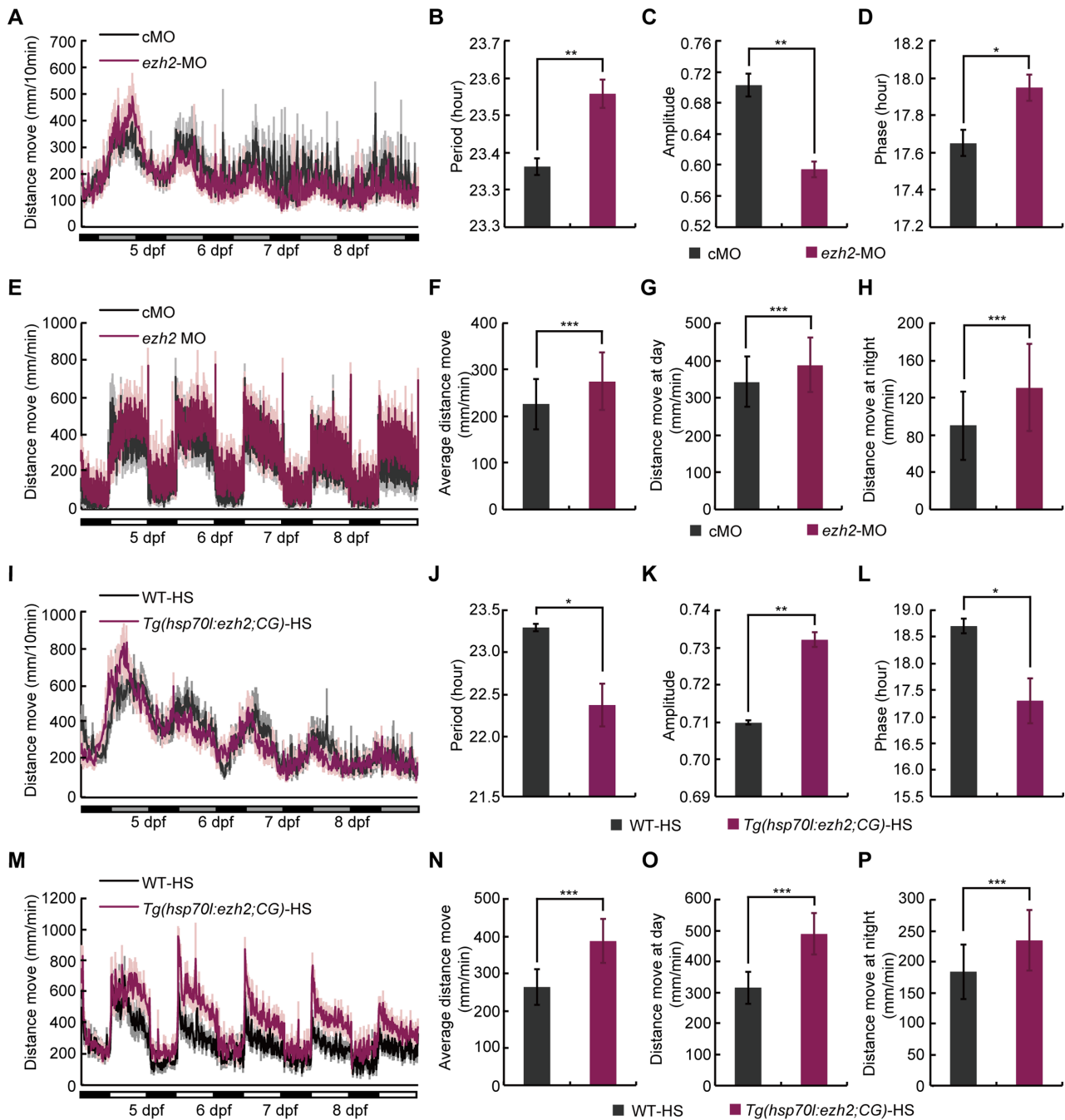


Figure 4. Altered locomotor rhythms in *ezh2* morphants and *ezh2*-overexpressing zebrafish larvae. (A–H) Locomotor activities were monitored and analyzed in *ezh2* morphants and control zebrafish larvae under DD (A–D) or LD (E–H) condition. The period (B), amplitude (C) and phase (D) under DD condition and total average moving distances (F), at day (G) and night (H) under LD conditions were shown. Student's *t*-test was conducted. * $P < 0.05$; ** $P < 0.01$; *** $P < 0.001$. (I–P) Locomotor assays were conducted in *ezh2*-overexpressing and control zebrafish larvae under LD (I–L) or LD (N–P) condition. The period (J), amplitude (K) and phase (L) under DD condition and total average moving distances (N), at day (O) and at night (P) under LD conditions were shown. Overexpression of *ezh2* was done with heat shock at 108 hpf (ZT12) for 1 h, and then locomotor assays were performed. Student's *t*-test was conducted. * $P < 0.05$, ** $P < 0.01$; *** $P < 0.001$.

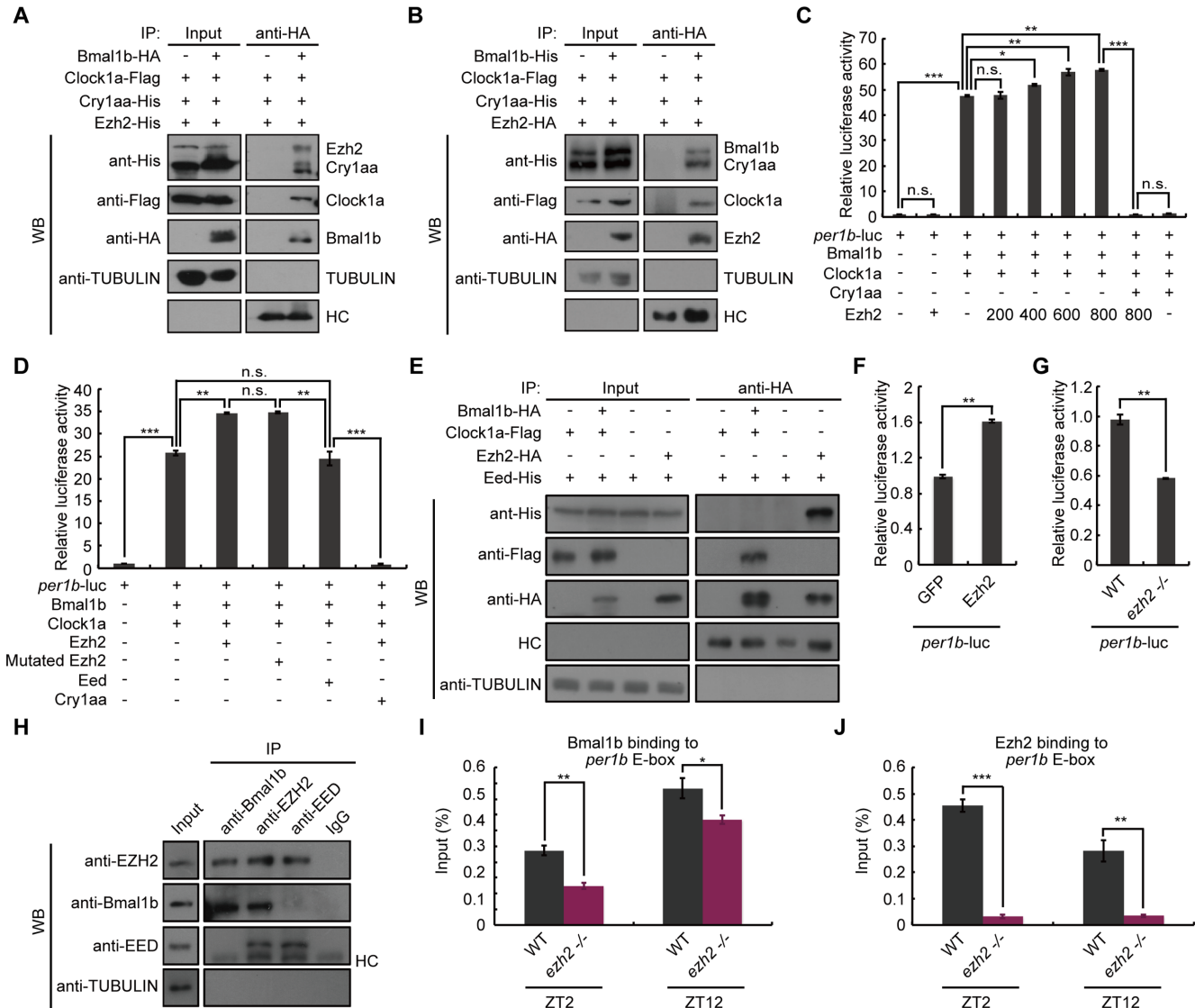


Figure 5. Zebrafish Ezh2 enhances expression of clock genes through binding to core clock components independent of its H3K27 methyltransferase activity. (A, B) Co-IP assays show that zebrafish Ezh2 complexes with Bmal1b, Clock1a, and Cry1aa. (C) Luciferase reporter assays show that zebrafish Ezh2 enhances transcription activities of Clock1a and Bmal1b in a dose-dependent manner. Co-transfection was performed as indicated, and luciferase activities were assayed 24 h after transfection. Experiments were performed in three independent experiments. Transactivation activities are expressed as fold increase over the control group. Values are expressed as means \pm S.D., $n = 3$. Student's *t*-test was conducted. * $P < 0.05$; ** $P < 0.01$; *** $P < 0.001$. (D) Luciferase reporter assays show that Ezh2 enhances expression of circadian clock genes independent of its H3K27 methyltransferase activity. Student's *t*-test was conducted. ** $P < 0.01$; *** $P < 0.001$. (E) Co-IP assays show that Clock1a and Bmal1b bind to Ezh2 but not to Eed. (F, G) *per1b-luc* expression was up-regulated in *ezh2*-overexpressing zebrafish embryos (F) and down-regulated in *ezh2*^{-/-} mutant zebrafish embryos (G). 50 pg of *per1b-luc* plasmid was injected into wild-type or *ezh2*^{-/-} mutant zebrafish embryos with or without 100 pg *ezh2* mRNA. Embryos were homogenized at 28 hpf and luciferase assays were performed. Student's *t*-test was conducted. ** $P < 0.01$. (H) Co-IP assays show that Bmal1b binds to Ezh2 in zebrafish. (I, J) ChIP-qPCR assays show that Bmal1b (I) and Ezh2 (J) bind to the E-box of the zebrafish *per1b* promoter region. Student's *t*-test was conducted. * $P < 0.05$; ** $P < 0.01$; *** $P < 0.001$.

qRT-PCR (Figure 6C). These results implicate that Ezh2 plays a pivotal role in hematopoiesis *in vivo*.

Ezh2 is essential for primitive hematopoiesis in zebrafish

To further investigate roles of Ezh2 in hematopoiesis, we performed blood cell staining and WISH. O-dianisidine staining shows that red blood cells are dramatically reduced in the *ezh2*^{-/-} mutant embryos at 33 hpf (Figure 7A and B). To determine whether the primitive hematopoiesis is af-

fected in *ezh2*^{-/-} mutant fish, we performed whole mount *in situ* hybridization using *gata1* (a marker for erythroid progenitors) (69–71), *pu.1* (a marker for myeloid progenitors) (72), *hbbe1* (a marker for erythroid cells) (73), *mpx* (a marker for granulocytes) (74), and *l-plastin* (a marker for macrophages) (75). Results show that *gata1* (Figure 7C and D) and *pu.1* (Figure 7E and F) are markedly reduced in the *ezh2*^{-/-} mutant ICM at 26 hpf, while *hbbe1* (Figure 7G and H), *mpx* (Figure 7I and J), and *l-plastin* (Figure 7K and L) are down-regulated in the *ezh2*^{-/-} mutant PBI at 28 hpf.

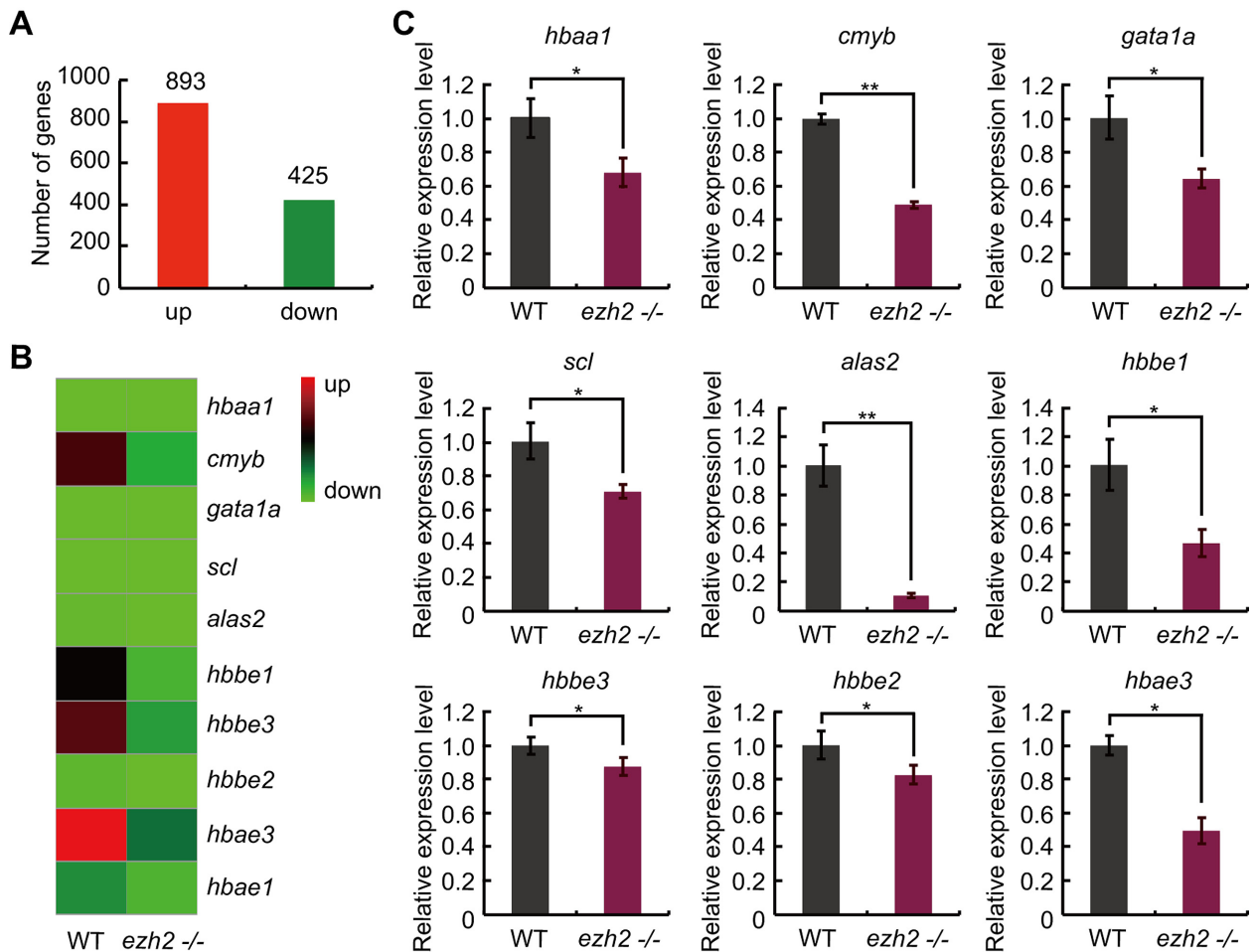


Figure 6. Disrupted expression of hematopoietic genes in *ezh2*^{-/-} mutant zebrafish revealed by transcriptome analysis. (A) Numbers of differentially expressed genes (DEGs) in *ezh2*^{-/-} mutant zebrafish at 28 hpf, revealed by transcriptome analysis. (B) Histogram of 10 hematopoietic DEGs in *ezh2*^{-/-} mutant zebrafish. Red and green colors represent up-regulation and down-regulation, respectively. (C) Nine out of 10 down-regulated hematopoietic genes revealed by transcriptome analysis are reconfirmed by independent qRT-PCR analysis. Three independent experiments were performed. Statistical analysis was performed using Student's *t*-test. **P* < 0.05; ***P* < 0.01.

In addition, primitive marker genes *gatal* (Supplementary Figure S13A and B) and *pu.1* (Supplementary Figure S13C and D) are also down-regulated in *ezh2* morphant embryos, consistent with the results observed in the *ezh2*^{-/-} mutant embryos.

To further visualize primitive hematopoiesis defects in *ezh2*^{-/-} mutant zebrafish, we crossed *ezh2*^{-/-} mutant zebrafish with transgenic zebrafish lines of several hematopoietic markers. Living imaging results show that loss of Ezh2 leads to reduced *gatal:dsRed* cells in the ICM at 24 hpf (Figure 7M and N) and 28 hpf (Figure 7O and P), reduced *mpx:eGFP* cells (Figure 7Q to T) and reduced *lyz:eGFP* cells (Figure 7U and V) in the trunk region at 28 hpf (Figure 7Q, R, U and V) and 48 hpf (Figure 7S and T). Together, these results suggest that Ezh2 is required for primitive hematopoiesis.

Ezh2 is required for definitive hematopoiesis and specification of HSCs in zebrafish

To investigate the role of Ezh2 in definitive hematopoiesis, we examined expression of *runx1* (76), *c-myb* (77), and

ikaros (78), markers for HSCs in the ventral wall of the dorsal aorta in *ezh2*^{-/-} mutant zebrafish by WISH. Results show that *runx1*, *c-myb*, and *ikaros* are dramatically reduced in the ventral wall of the dorsal aorta in *ezh2*^{-/-} mutant embryos at 28 hpf (Figure 8A to F), suggesting that the specification of HSCs is affected in *ezh2*^{-/-} mutant zebrafish. We also examined expression of markers for lymphoid cells in *ezh2*^{-/-} mutant zebrafish. WISH results show that *ikaros*, *lck* (79), and *rag-1* (80) all lose their expression domains in *ezh2*^{-/-} mutant zebrafish at 96 hpf (Figure 7G–L), implicating the lymphoid defects in *ezh2*^{-/-} mutant zebrafish. Further, definitive hematopoiesis markers *runx1* (Supplementary Figure S13E and F) and *cmyb* (Supplementary Figure S13G and H) are all down-regulated in *ezh2* morphant embryos. *In vivo* living image results show that *cmyb:eGFP* cells (Figure 8M to P) and *coro1a:eGFP* cells (Figure 8Q–T) are reduced in the ICM (Figure 8M, N, Q and R) and the thymus (Figure 8O, P, S and T) in *ezh2*^{-/-} mutant zebrafish. Together, these results suggest that Ezh2 plays a critical role in definitive hematopoiesis and specification of HSCs in zebrafish.

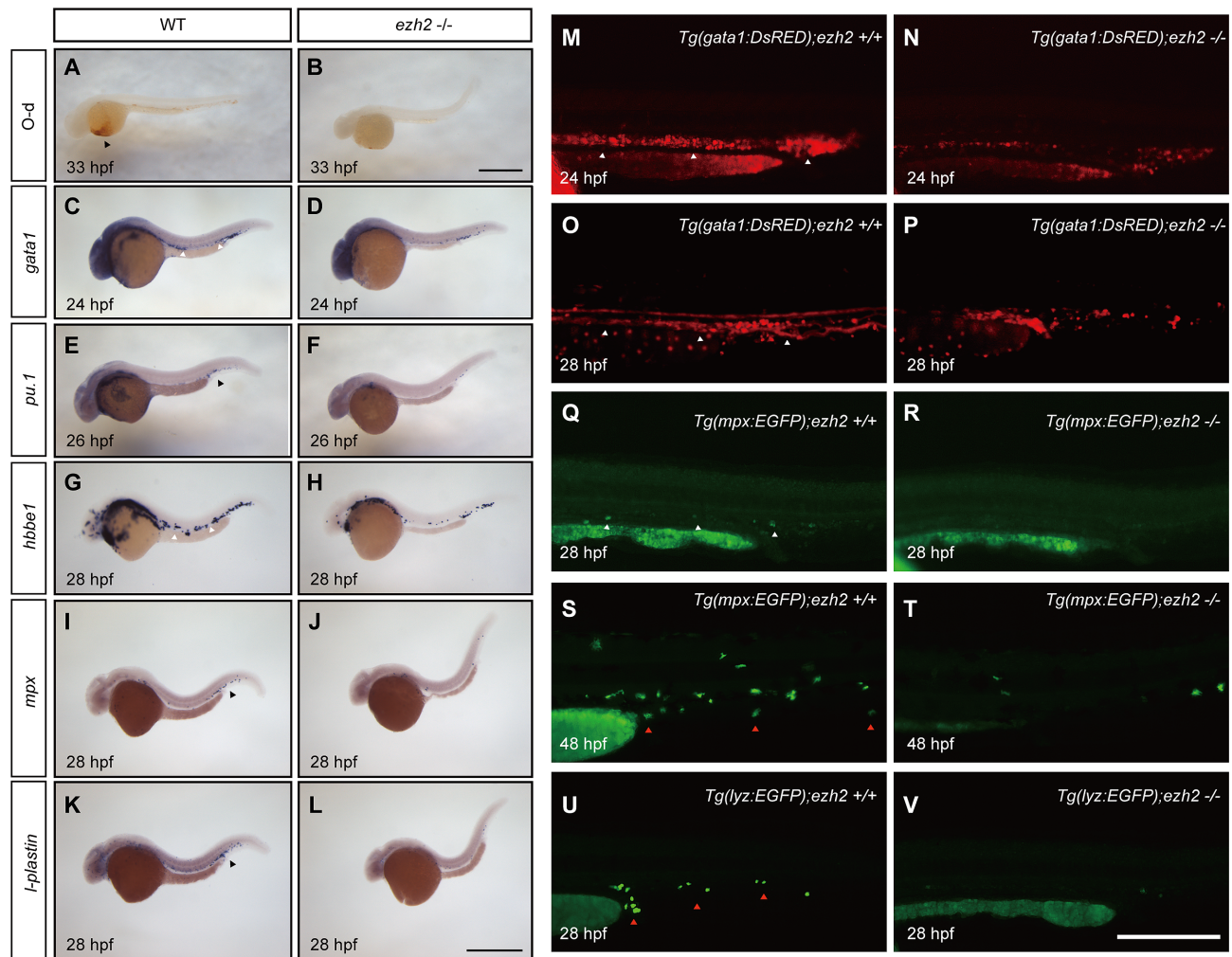


Figure 7. Primitve hematopoiesis is disrupted in *ezh2*^{-/-} mutant zebrafish. (A, B) O-dianisidine (O-d) staining of wild-type sibling (A) and *ezh2*^{-/-} mutant fish (B) at 33 hpf. Black arrowhead indicates hemoglobin-staining, which is significantly reduced in *ezh2*^{-/-} mutant zebrafish. (C–L) *In situ* hybridization of wild-type (C, E, G, I and K) and *ezh2*^{-/-} mutant embryos (D, F, H, J and L) using probes of *gata1* (C, D), *pu.1* (E, F), *hbbe1* (G, H), *mpx* (I, J), *l-plastin* (K, L) at 26 hpf (C–F) and 28 hpf (G–L), respectively. White arrowheads in (C) and (G) indicate ICM (Intermediate cell mass) and black arrowheads in (E, I and K) PBI (Posterior blood island). Scale bar, 0.25 mm. (M–P) Images of *gata1:dsRed* cells in WT (M, O) and *ezh2*^{-/-} mutant (N, P) fish at 24 hpf (M, N) and 28 hpf (O, P). (Q–T) Images of *mpx:eGFP* cells in wild-type (Q, S) and *ezh2*^{-/-} mutant (R, T) fish at 28 hpf (Q, R) and 48 hpf (S, T). (U, V) Images of *lyz:eGFP* cells in wild-type (U) and *ezh2*^{-/-} mutant (V) fish at 28 hpf. White arrowheads in (M–R) indicate ICM and red arrowheads in (S–V) PBI. Scale bar in (M–V), 0.25 mm. All images shown are lateral view, anterior to left.

Specification and development of hemangioblasts and vascular endothelial cells are not affected in *ezh2*^{-/-} mutant zebrafish during early development

Because HSCs and endothelial cells (ECs) are both derived from hemangioblast (40,81), we next examined expression of hemangioblast markers. WISH shows that expression of *flila*, a marker for hemangioblasts (77) at zebrafish early development, is not altered in *ezh2*^{-/-} mutant zebrafish in comparison with that of its wild-type siblings at 80% epiboly (Supplementary Figure S14A and B). *scl*, a marker for hemangioblasts (82), HSCs, and angioblasts, has the same expression pattern in *ezh2*^{-/-} mutant zebrafish as in its wide-type siblings at 80% epiboly (Supplementary Figure S14C and D). We then examined endothelial development using markers *flila* and *flk1*. Results show that the vasculature develops normally in *ezh2*^{-/-} mutant zebrafish at 24

hpf (Supplementary Figure S14E to H). These results indicate that specification and development of hemangioblasts and ECs are not affected during early development of *ezh2*^{-/-} mutant embryos in spite of its hematopoietic defects.

Hematopoietic genes are regulated by the circadian clock and Ezh2 complex

The results that *ezh2* is controlled by the circadian clock and hematopoietic genes are down-regulated in *ezh2*^{-/-} mutant fish led us to hypothesize that most, if not all, hematopoietic genes, are rhythmically expressed. To examine this hypothesis, we first analyzed approximately 2.5-kb 5' promoter regions of hematopoietic genes and found that there are E-boxes in the *cmyb* and *lck* contain promoter regions. qRT-PCR results show that *cymb* (Figure 9A and B) and *lck* (Figure 9C and D) are rhythmically expressed in ze-

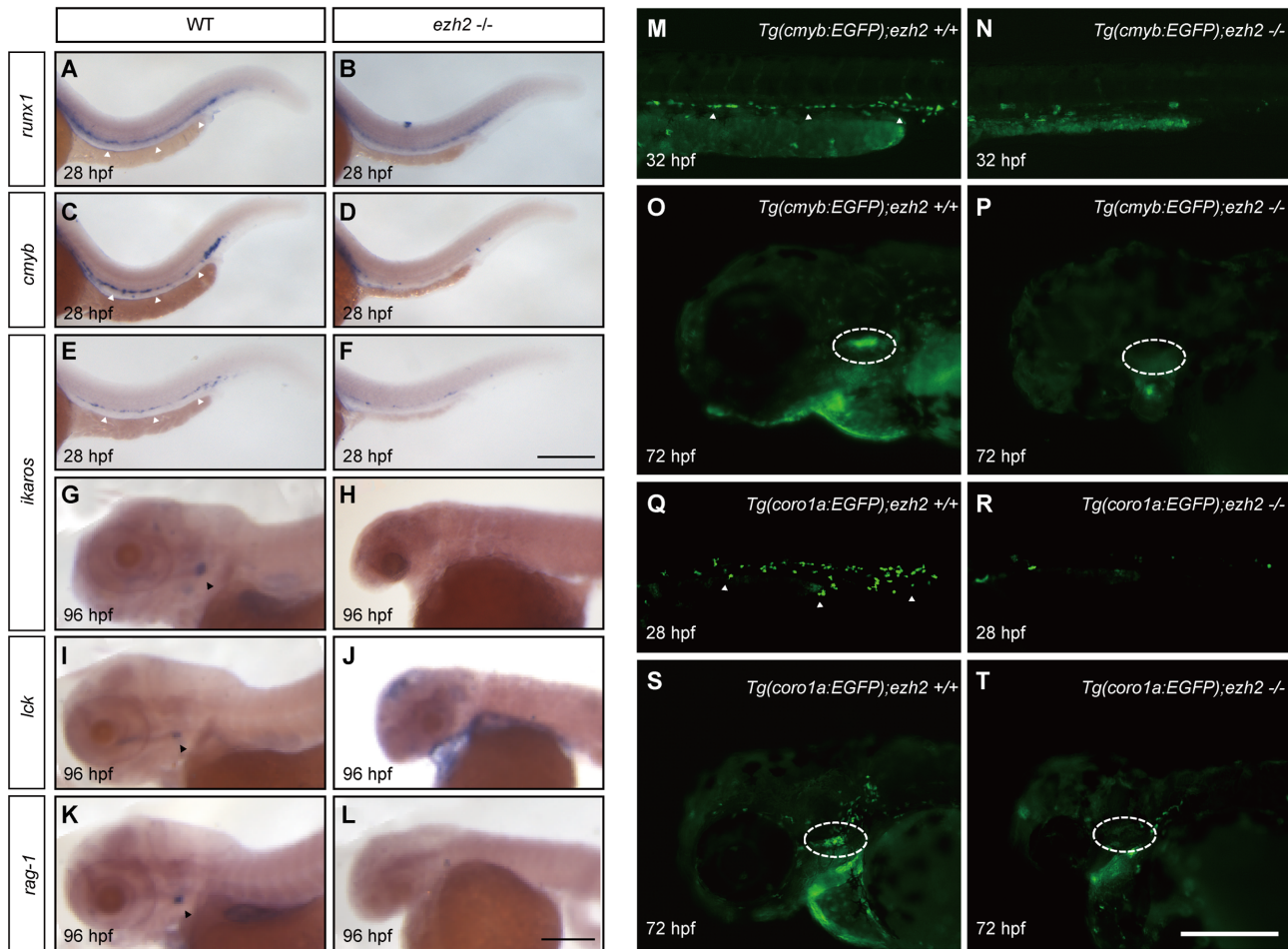


Figure 8. Definitive hematopoiesis is disrupted in *ezh2*^{-/-} mutant zebrafish. (A–L) *In situ* hybridization of WT sibling (A, C, E, G, I and K) and *ezh2*^{-/-} mutant embryos or larvae (B, D, F, G, J and L) using probes of *runx1* (A, B), *cmyb* (C, D), *ikaros* (E, H), *lck* (I, J), *rag-1* (K, L) at 28 hpf (A, F) and 96 hpf (G, L), respectively. White arrowheads indicate ICM in A, C and E and black arrowheads the thymus in G, I and K. Scale bar, 0.25 mm. (M–P) Images of *cmyb:eGFP* cells in wild-type (M, O) and *ezh2*^{-/-} mutant (N, P) fish at 32 hpf (M, N) and 72 hpf (O, P). (Q–T) Images of *coro1a:eGFP* cells in wild-type (Q, S) and *ezh2*^{-/-} mutant (R, T) fish at 28 hpf (Q, R) and 72 hpf (S, T). White arrowheads indicate ICM in M, N, Q and R and dashed circle the thymus in O, P, S and T. Scale bar in (M–T), 0.25 mm. All images shown are lateral view, anterior to left.

brafish larvae under both DD and LD conditions but are down-regulated in *ezh2*^{-/-} mutant zebrafish, which were also observed in *ezh2* morphants (Figure 9E and F). In contrast, overexpressing *ezh2* by mRNA injection up-regulates these genes (Figure 9G and H). ChIP-qPCR results showed that Bmal1b and Ezh2 rhythmically bind to the E-boxes of *cmyb* (Figure 9I, J and Supplemental S1D) and *lck* (Figure 9K, L and Supplemental S1E). Furthermore, luciferase reporter assays showed that Bmal1b-Clock1a activates *cmyb*-luc (Figure 9M) and *lck*-luc (Figure 9N), which is enhanced by Ezh2 (Figure 9M and N). Taken together, these results suggest that both the circadian clock and Ezh2 play regulatory roles in zebrafish hematopoiesis.

DISCUSSION

Regulation of *EZH2* expression has been studied extensively in different types of human cancers (18). For instance, E2Fs activate *EZH2* expression via binding to its promoter (83). EWS-FLI1 and NF- κ B2 activate *EZH2*, while SNF5 represses it (64,84,85). It was also reported that

EZH2 is transcriptionally induced by Estradiol, Bisphenol-A, and Diethylstilbestrol through Estrogen-response elements (EREs) (65). But how it is regulated in normal physiology in animals still remains unclear. In animals, ~43% of transcripts show circadian expression (86,87). However, whether *EZH2* is regulated by the circadian clock is unknown to date. Here we show that zebrafish *ezh2* is rhythmically expressed but up-regulated in *per1b*^{-/-} and *rev-erba*^{-/-} mutants under both DD and LD condition. Luciferase and ChIP-qPCR reveal that *ezh2* is regulated directly by the circadian clock through E-box and RORE. However, statistical analysis of qRT-PCR data shows that *ezh2* still remains rhythmic with reduced amplitudes in *per1b*^{-/-} mutant fish under LD condition and in *rev-erba*^{-/-} mutant under DD condition, indicating that both *Per1b* and *Rev-erba* play large roles in the amplitude of *ezh2* expression. In addition, the expression level of *ezh2* appears gradually decreased during development (Figure 1A and B), suggesting that *ezh2* is also affected by unknown developmental cues. A previous study showed that transcription factor CLOCK

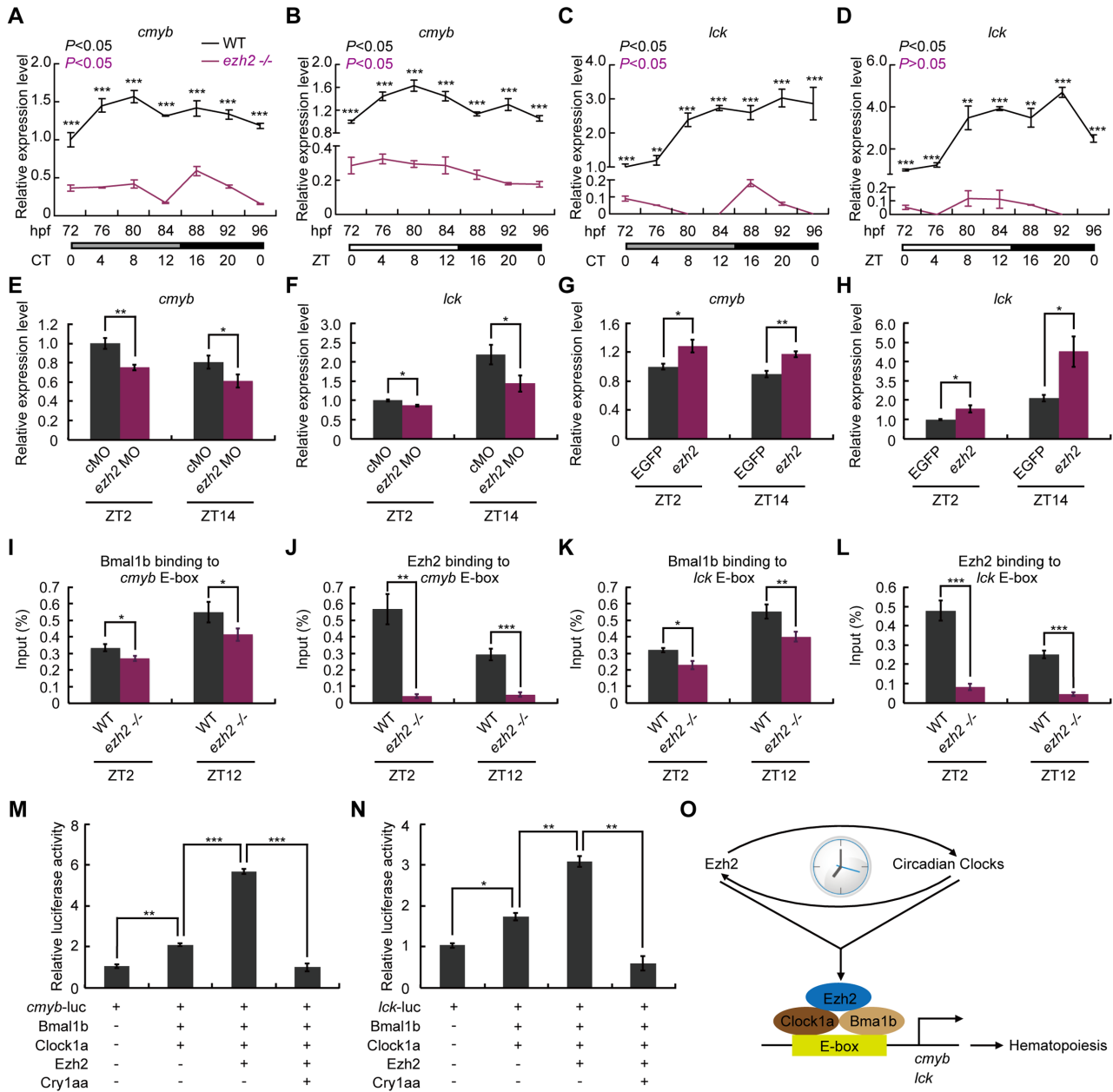


Figure 9. Ezh2 and the circadian clock regulate zebrafish hematopoietic genes. (A–D) qRT-PCR analysis of *cmyb* (A, B) and *lck* (C, D) in WT and *ezh2*^{-/-} mutant under DD (A, C) and LD (B, D) conditions. Three independent experiments were conducted. Rhythmic mRNA expression was analyzed with the JTK-CYCLE method. ADJP for adjusted minimal *P*-values ($P < 0.05$). Two-way ANOVA with Tukey's *post hoc* test was conducted, $**P < 0.01$; $***P < 0.005$. (E, F) Down-regulation of *cmyb* (E) and *lck* (F) in *ezh2* morphants. Student's *t*-test was conducted. $*P < 0.05$; $**P < 0.01$. (G, H) Up-regulation of *cmyb* (G) and *lck* (H) in *ezh2*-overexpressing zebrafish. Student's *t*-test was conducted. $*P < 0.05$; $**P < 0.01$. (I–L) ChIP-qPCR results show that Bmal1b and Ezh2 bind to E-boxes in the promoters of *cmyb* (I, J) and *lck* (K, L). Student's *t*-test was conducted. $*P < 0.05$; $**P < 0.01$; $***P < 0.001$. (M, N) Luciferase reporter assays show that *cmyb-luc* (M) and *lck-luc* (N) are activated by Bmal1b-Clock1a, respectively, and Ezh2 enhances Bmal1b-Clock1a transcription activities. Three independent experiments were performed. Statistical analysis was performed using Student's *t*-test. $*P < 0.05$; $**P < 0.01$; $***P < 0.005$. (O) A model for regulation of hematopoiesis by Ezh2 and the circadian clock in zebrafish. Zebrafish *ezh2* is controlled directly by the circadian clock and contributes to circadian regulation by binding to the clock complex. The Ezh2 and clock complex controls hematopoiesis through directly regulating hematopoietic genes, *cmyb* and *lck*, mediated by E-boxes, respectively.

protein, an essential component of the mammalian circadian system, is a histone acetyltransferase (88). This and our results reveal that the circadian clock could regulate histone remodeling at both transcriptional and translational level.

Posttranslational modifications of histones are essential for transcriptional regulation of gene expression. Histone modification also has found to be evolved as an important mechanism at the core circadian machinery (9). EZH2 was shown to be required for the mouse liver clock *in vitro* (26). However, because loss of *Ezh2* results in lethality during mouse early development (19), effects of EZH2 on clock gene expression and locomotor rhythmicity in live animals are unknown. Here we recovered an ENU-induced *ezh2*^{-/-} mutant zebrafish that can live up to seven days. Key circadian clock genes are down-regulated in the *ezh2*^{-/-} mutant zebrafish. Knockdown or overexpression of *ezh2* alters zebrafish larval locomotor rhythms. Moreover, consistent with mice EZH2 (26), zebrafish *Ezh2* contributes to circadian regulation through binding to the core clock components and regulates clock genes by E-box. Interestingly, we found that zebrafish *Ezh2* enhances clock function independent of polycomb repressive complex 2, differing from mice EZH2 that augments the repressive action of CRY1 (26). Our data suggest that zebrafish *Ezh2* and mice EZH2 contribute to circadian function through different mechanisms.

EZH2 was shown to play pivotal roles in stem cell maintenance and have a dual role as either oncogene or tumor-suppressor gene, depending on gene dosages and cell context progression of several types of tumors, including breast and prostate cancers (18,20,89). EZH2 also is important for normal and malignant hematopoiesis (28,29). However, due to embryonic lethality of *Ezh2*^{-/-} mutant mice, whether EZH2 regulates hematopoiesis in early development remains unclear. We found that both primitive and definitive hematopoiesis is affected in *ezh2*^{-/-} mutant zebrafish, as evidenced that loss of *Ezh2* results in reduced numbers of erythroid cells, granulocytes, macrophages, T cells, and HSCs in live zebrafish. These are not likely due to developmental delay because the mutant fish embryos appear normal outwardly before 28 hpf. Our results are consistent with a previous study that knocking out *Ezh2* specifically in the mouse liver impaired expansion of HSCs and reduced the number of megakaryocyte-erythroid progenitors, but moderately reduced common myeloid progenitors and granulocyte-macrophage progenitors (90).

Circadian rhythms are highly conserved among organisms ranging from prokaryotes to humans, to maintain coordination with the daily changes of light and temperature. However, little is known about circadian control of hematopoiesis. It has been reported that hematopoietic stem cell release is regulated by circadian oscillations (91). Circadian clock gene *Bmal1* regulates diurnal oscillations of Ly6C^{hi} inflammatory monocytes (92). EZH2 was found to be overexpressed in natural killer/T-cell lymphoma (NKTL), and directly activates *CCND1* in NKTL without histone methyltransferase activity (93). We found that *cmyb* and *lck* involved in hematopoiesis display rhythmic expression, which are down-regulated in *ezh2*^{-/-} mutant zebrafish; importantly, zebrafish *Bmal1b* and *Ezh2* regulate *cmyb* and *lck* through directly binding to the E-box in their promoters, indicating that *Ezh2* promotes nor-

mal hematopoiesis via directly enhancing key hematopoietic marker genes in zebrafish. However, even though we observed rhythmic expression of other important hematopoietic genes, for instance, *gata1a*, *pu.1*, *mpx* and *ikaros*, exactly how *Ezh2* and the circadian clock regulate them would need to be investigated in the future. Nonetheless, our results reveal that the circadian clock modulates hematopoiesis in an intricate manner, i.e. the circadian clock regulates *ezh2* directly and the *Ezh2*-circadian clock complex in turn regulates hematopoiesis (Figure 90).

In summary, zebrafish *ezh2* is regulated directly by the circadian clock. *Ezh2* promotes clock function and hematopoiesis independent of its histone methyltransferase activity.

DATA AVAILABILITY

The data was deposited into NCBI Gene Expression Omnibus, GEO accession number GSE103913.

SUPPLEMENTARY DATA

Supplementary Data are available at NAR Online.

ACKNOWLEDGEMENTS

We thank Feng Liu and Wenqing Zhang for sharing plasmids of *pu.1*, *hbbe1*, *mpx*, *plastin*, *c-myb*, *runx1*, *ikaros*, *lck* and *rag-1*; Leonard Zon, Philip Crosie, Zilong Wen, Shuo Lin and Stephen Renshaw for sharing transgenic lines of *Tg(cmyb:EGFP)*, *Tg(lyz:EGFP)*, *Tg(coro1a:EGFP)*, *Tg(gatal:DsRED)* and *Tg(mpx:EGFP)*; and Mishra Kumar for carefully reading the manuscript.

Author contributions: Y.Z. and H.W. designed the study; Y.Z., Q.Y., C.C. and M.W. performed experiments; Y.Z. and H.W. analyzed data and wrote the manuscript.

FUNDING

National Basic Research Program of China (973 Program) [2012CB947600]; National Natural Science Foundation of China (NSFC) [31200877, 31030062, 81570171]; Jiangsu Planned Projects for Postdoctoral Research Funds [1401013A]; Jiangsu Distinguished Professorship Program [SR13400111]; Natural Science Foundation of Jiangsu Province [BK2012052]; Priority Academic Program Development (PAPD) of Jiangsu Higher Education Institutions [YX13400214]; High-Level Innovative Team of Jiangsu Province, and the '333' project of Jiangsu Province [BRA2015328]. Funding for open access charge: National Basic Research Program of China (973 Program) [2012CB947600]; National Natural Science Foundation of China (NSFC) [31200877, 31030062, 81570171]; Jiangsu Planned Projects for Postdoctoral Research Funds [1401013A]; Jiangsu Distinguished Professorship Program [SR13400111]; Natural Science Foundation of Jiangsu Province [BK2012052]; Priority Academic Program Development (PAPD) of Jiangsu Higher Education Institutions [YX13400214]; High-Level Innovative Team of Jiangsu Province, and the '333' project of Jiangsu Province [BRA2015328].

Conflict of interest statement. None declared.

REFERENCES

- Takahashi, J.S. (2017) Transcriptional architecture of the mammalian circadian clock. *Nat. Rev. Genet.*, **18**, 164–179.
- Klein, D.C., Moore, R.Y. and Reppert, S.M. (1991) *Suprachiasmatic Nucleus: The Mind's Clock*. Oxford University Press, NY.
- Yamazaki, S., Numano, R., Abe, M., Hida, A., Takahashi, R., Ueda, M., Block, G.D., Sakaki, Y., Menaker, M. and Tei, H. (2000) Resetting central and peripheral circadian oscillators in transgenic rats. *Science*, **288**, 682–685.
- Lee, C., Etchegaray, J.P., Cagampang, F.R., Loudon, A.S. and Reppert, S.M. (2001) Posttranslational mechanisms regulate the mammalian circadian clock. *Cell*, **107**, 855–867.
- Gekakis, N., Staknis, D., Nguyen, H.B., Davis, F.C., Wilsbacher, L.D., King, D.P., Takahashi, J.S. and Weitz, C.J. (1998) Role of the CLOCK protein in the mammalian circadian mechanism. *Science*, **280**, 1564–1569.
- Kume, K., Zylka, M.J., Sriram, S., Shearman, L.P., Weaver, D.R., Jin, X., Maywood, E.S., Hastings, M.H. and Reppert, S.M. (1999) mCRY1 and mCRY2 are essential components of the negative limb of the circadian clock feedback loop. *Cell*, **98**, 193–205.
- Preitner, N., Damiola, F., Lopez-Molina, L., Zakany, J., Duboule, D., Albrecht, U. and Schibler, U. (2002) The orphan nuclear receptor REV-ERB α controls circadian transcription within the positive limb of the mammalian circadian oscillator. *Cell*, **110**, 251–260.
- Ripperger, J.A. and Merrow, M. (2011) Perfect timing: epigenetic regulation of the circadian clock. *FEBS Lett.*, **585**, 1406–1411.
- Etchegaray, J.P., Lee, C., Wade, P.A. and Reppert, S.M. (2003) Rhythmic histone acetylation underlies transcription in the mammalian circadian clock. *Nature*, **421**, 177–182.
- Naruse, Y., Oh-hashi, K., Iijima, N., Naruse, M., Yoshioka, H. and Tanaka, M. (2004) Circadian and light-induced transcription of clock gene Per1 depends on histone acetylation and deacetylation. *Mol. Cell Biol.*, **24**, 6278–6287.
- Brown, S.A., Ripperger, J., Kadener, S., Fleury-Olela, F., Vilbois, F., Rosbash, M. and Schibler, U. (2005) PERIOD1-associated proteins modulate the negative limb of the mammalian circadian oscillator. *Science*, **308**, 693–696.
- Ripperger, J.A. and Schibler, U. (2006) Rhythmic CLOCK–BMAL1 binding to multiple E-box motifs drives circadian Dbp transcription and chromatin transitions. *Nat. Genet.*, **38**, 369–374.
- Jones, M.A., Covington, M.F., DiTacchio, L., Vollmers, C., Panda, S. and Harmer, S.L. (2010) Jumonji domain protein JMJD5 functions in both the plant and human circadian systems. *Proc. Natl. Acad. Sci. U.S.A.*, **107**, 21623–21628.
- Lu, S.X., Knowles, S.M., Webb, C.J., Celaya, R.B., Cha, C., Siu, J.P. and Tobin, E.M. (2011) The Jumonji C domain-containing protein JMJD3 regulates period length in the Arabidopsis circadian clock. *Plant Physiol.*, **155**, 906–915.
- Paro, R. and Harte, P.J. (1996) The role of Polycomb group and trithorax group chromatin complexes in the maintenance of determined cell states. In: Russo, VEA, Martienssen, RA and Riggs, AD (eds). *Epigenetic Mechanisms of Gene Regulation*, NY: Cold Spring Harbor Laboratory Press, pp. 507–528.
- Lund, A.H. and van Lohuizen, M. (2004) Polycomb complexes and silencing mechanisms. *Curr. Opin. Cell Biol.*, **16**, 239–246.
- Cao, R., Wang, L., Wang, H., Xia, L., Erdjument-Bromage, H., Tempst, P., Jones, R.S. and Zhang, Y. (2002) Role of histone H3 lysine 27 methylation in Polycomb-group silencing. *Science*, **298**, 1039–1043.
- Chang, C.J. and Hung, M.C. (2012) The role of EZH2 in tumour progression. *Br. J. Cancer*, **106**, 243–247.
- O'Carroll, D., Erhardt, S., Pagani, M., Barton, S.C., Surani, M.A. and Jenuwein, T. (2001) The polycomb-group gene Ezh2 is required for early mouse development. *Mol. Cell Biol.*, **21**, 4330–4336.
- Kim, K.H. and Roberts, C.W. (2016) Targeting EZH2 in cancer. *Nat. Med.*, **22**, 128–134.
- Lee, S.T., Li, Z., Wu, Z., Aau, M., Guan, P., Karuturi, R.K., Liou, Y.C. and Yu, Q. (2011) Context-specific regulation of NF- κ B target gene expression by EZH2 in breast cancers. *Mol. Cell*, **43**, 798–810.
- LaJunesse, D. and Shearn, A. (1996) E(z): a polycomb group gene or a trithorax group gene? *Development*, **122**, 2189–2197.
- Strutt, H., Cavalli, G. and Paro, R. (1997) Co-localization of Polycomb protein and GAGA factor on regulatory elements responsible for the maintenance of homeotic gene expression. *EMBO J.*, **16**, 3621–3632.
- Cavalli, G. (2012) Molecular biology. EZH2 goes solo. *Science*, **338**, 1430–1431.
- Xu, K., Wu, Z.J., Groner, A.C., He, H.H., Cai, C., Lis, R.T., Wu, X., Stack, E.C., Loda, M., Liu, T. et al. (2012) EZH2 oncogenic activity in castration-resistant prostate cancer cells is Polycomb-independent. *Science*, **338**, 1465–1469.
- Etchegaray, J.P., Yang, X., DeBruyne, J.P., Peters, A.H., Weaver, D.R., Jenuwein, T. and Reppert, S.M. (2006) The polycomb group protein EZH2 is required for mammalian circadian clock function. *J. Biol. Chem.*, **281**, 21209–21215.
- Tang, Q., Cheng, B., Xie, M., Chen, Y., Zhao, J., Zhou, X. and Chen, L. (2017) Circadian clock gene Bmal1 inhibits tumorigenesis and increases paclitaxel sensitivity in tongue squamous cell carcinoma. *Cancer Res.*, **77**, 532–544.
- Lund, K., Adams, P.D. and Copland, M. (2014) EZH2 in normal and malignant hematopoiesis. *Leukemia*, **28**, 44–49.
- Herviou, L., Cavalli, G., Cartron, G., Klein, B. and Moreaux, J. (2016) EZH2 in normal hematopoiesis and hematological malignancies. *Oncotarget*, **7**, 2284–2296.
- Su, I.H., Basavaraj, A., Krutchinsky, A.N., Hobert, O., Ullrich, A., Chait, B.T. and Tarakhovskiy, A. (2003) Ezh2 controls B cell development through histone H3 methylation and Igh rearrangement. *Nat. Immunol.*, **4**, 124–131.
- Roy, A., Basak, N.P. and Banerjee, S. (2012) Notch1 intracellular domain increases cytoplasmic EZH2 levels during early megakaryopoiesis. *Cell Death Dis.*, **3**, e380.
- Ross, J., Mavoungou, L., Bresnick, E.H. and Milot, E. (2012) GATA-1 utilizes Ikaros and polycomb repressive complex 2 to suppress Hes1 and to promote erythropoiesis. *Mol. Cell Biol.*, **32**, 3624–3638.
- Lessard, J., Baban, S. and Sauvageau, G. (1998) Stage-specific expression of polycomb group genes in human bone marrow cells. *Blood*, **91**, 1216–1224.
- Fukuyama, T., Otsuka, T., Shigematsu, H., Uchida, N., Arima, F., Ohno, Y., Iwasaki, H., Fukuda, T. and Niho, Y. (2000) Proliferative involvement of ENX-1, a putative human polycomb group gene, in haematopoietic cells. *Br. J. Haematol.*, **108**, 842–847.
- Herrera-Merchan, A., Arranz, L., Ligos, J.M., de Molina, A., Dominguez, O. and Gonzalez, S. (2012) Ectopic expression of the histone methyltransferase Ezh2 in haematopoietic stem cells causes myeloproliferative disease. *Nat. Commun.*, **3**, 623.
- Vatine, G., Vallone, D., Gothif, Y. and Foulkes, N.S. (2011) It's time to swim! Zebrafish and the circadian clock. *FEBS Lett.*, **585**, 1485–1494.
- Vallone, D., Lahiri, K., Dickmeis, T. and Foulkes, N.S. (2007) Start the clock! Circadian rhythms and development. *Dev. Dyn.*, **236**, 142–155.
- Wang, M.Y., Huang, G.D. and Wang, H. (2012) [Advances in the zebrafish circadian clock mechanisms]. *Yi chuan = Hereditas*, **34**, 1133–1143.
- Zhong, Z., Wang, M., Huang, G., Zhang, S. and Wang, H. (2017) Molecular genetic and genomic analyses of zebrafish circadian rhythmicity. Kumar, V (ed). *Biological Timekeeping: Clocks, Rhythms and Behaviour*, Springer (India) Pvt. Ltd., New Delhi, pp. 193–209.
- de Jong, J.L. and Zon, L.I. (2005) Use of the zebrafish system to study primitive and definitive hematopoiesis. *Annu. Rev. Genet.*, **39**, 481–501.
- Huang, J., Zhong, Z., Wang, M., Chen, X., Tan, Y., Zhang, S., He, W., He, X., Huang, G., Lu, H. et al. (2015) Circadian modulation of dopamine levels and dopaminergic neuron development contributes to attention deficiency and hyperactive behavior. *J. Neurosci.*, **35**, 2572–2587.
- Huang, G., Zhang, F., Ye, Q. and Wang, H. (2016) The circadian clock regulates autophagy directly through the nuclear hormone receptor Nr1d1/Rev-erb α and indirectly via Cebpb/(C/ebp β) in zebrafish. *Autophagy*, **12**, 1292–1309.
- Traver, D., Paw, B.H., Poss, K.D., Penberthy, W.T., Lin, S. and Zon, L.I. (2003) Transplantation and in vivo imaging of multilineage engraftment in zebrafish bloodless mutants. *Nat. Immunol.*, **4**, 1238–1246.
- Renshaw, S.A., Loynes, C.A., Trushell, D.M., Elworthy, S., Ingham, P.W. and Whyte, M.K. (2006) A transgenic zebrafish model of neutrophilic inflammation. *Blood*, **108**, 3976–3978.

45. Hall, C., Flores, M.V., Storm, T., Crosier, K. and Crosier, P. (2007) The zebrafish lysozyme C promoter drives myeloid-specific expression in transgenic fish. *BMC Dev. Biol.*, **7**, 42.
46. North, T.E., Goessling, W., Walkley, C.R., Lengerke, C., Kopani, K.R., Lord, A.M., Weber, G.J., Bowman, T.V., Jang, I.H., Grosser, T. et al. (2007) Prostaglandin E2 regulates vertebrate haematopoietic stem cell homeostasis. *Nature*, **447**, 1007–1011.
47. Li, L., Yan, B., Shi, Y.Q., Zhang, W.Q. and Wen, Z.L. (2012) Live imaging reveals differing roles of macrophages and neutrophils during zebrafish tail fin regeneration. *J. Biol. Chem.*, **287**, 25353–25360.
48. Kuzmichev, A., Nishioka, K., Erdjument-Bromage, H., Tempst, P. and Reinberg, D. (2002) Histone methyltransferase activity associated with a human multiprotein complex containing the Enhancer of Zeste protein. *Genes Dev.*, **16**, 2893–2905.
49. Joshi, P., Carrington, E.A., Wang, L., Ketel, C.S., Miller, E.L., Jones, R.S. and Simon, J.A. (2008) Dominant alleles identify SET domain residues required for histone methyltransferase of Polycomb repressive complex 2. *J. Biol. Chem.*, **283**, 27757–27766.
50. Sun, X.J., Xu, P.F., Zhou, T., Hu, M., Fu, C.T., Zhang, Y., Jin, Y., Chen, Y., Chen, S.J., Huang, Q.H. et al. (2008) Genome-wide survey and developmental expression mapping of zebrafish SET domain-containing genes. *PLoS One*, **3**, e1499.
51. Kettleborough, R.N., Busch-Nentwich, E.M., Harvey, S.A., Dooley, C.M., de Bruijn, E., van Eeden, F., Sealy, I., White, R.J., Herd, C., Nijman, I.J. et al. (2013) A systematic genome-wide analysis of zebrafish protein-coding gene function. *Nature*, **496**, 494–497.
52. Kwan, K.M., Fujimoto, E., Grabher, C., Mangum, B.D., Hardy, M.E., Campbell, D.S., Parant, J.M., Yost, H.J., Kanki, J.P. and Chien, C.B. (2007) The Tol2kit: a multisite gateway-based construction kit for 2007 transposon transgenesis constructs. *Dev. Dyn.*, **236**, 3088–3099.
53. Zhong, Y., Lu, L., Zhou, J., Li, Y., Liu, Y., Clemmons, D.R. and Duan, C. (2011) IGF binding protein 3 exerts its ligand-independent action by antagonizing BMP in zebrafish embryos. *J. Cell Sci.*, **124**, 1925–1935.
54. Wang, H., Zhou, Q., Kesinger, J.W., Norris, C. and Valdez, C. (2007) Heme regulates exocrine peptidase precursor genes in zebrafish. *Exp. Biol. Med.*, **232**, 1170–1180.
55. Livak, K.J. and Schmittgen, T.D. (2001) Analysis of relative gene expression data using real-time quantitative PCR and the 2^{-Delta}Delta C(T) Method. *Methods*, **25**, 402–408.
56. Li, Y., Xiang, J. and Duan, C. (2005) Insulin-like growth factor-binding protein-3 plays an important role in regulating pharyngeal skeleton and inner ear formation and differentiation. *J. Biol. Chem.*, **280**, 3613–3620.
57. Appelbaum, L., Wang, G., Yokogawa, T., Skariah, G.M., Smith, S.J., Mourrain, P. and Mignot, E. (2010) Circadian and homeostatic regulation of structural synaptic plasticity in hypocretin neurons. *Neuron*, **68**, 87–98.
58. Prober, D.A., Rihel, J., Onah, A.A., Sung, R.J. and Schier, A.F. (2006) Hypocretin/orexin overexpression induces an insomnia-like phenotype in zebrafish. *J. Neurosci.*, **26**, 13400–13410.
59. Grabherr, M.G., Haas, B.J., Yassour, M., Levin, J.Z., Thompson, D.A., Amit, I., Adiconis, X., Fan, L., Raychowdhury, R., Zeng, Q. et al. (2011) Full-length transcriptome assembly from RNA-Seq data without a reference genome. *Nat. Biotechnol.*, **29**, 644–652.
60. Trapnell, C., Williams, B.A., Pertea, G., Mortazavi, A., Kwan, G., van Baren, M.J., Salzberg, S.L., Wold, B.J. and Pachter, L. (2010) Transcript assembly and quantification by RNA-Seq reveals unannotated transcripts and isoform switching during cell differentiation. *Nat. Biotechnol.*, **28**, 511–515.
61. Young, M.D., Wakefield, M.J., Smyth, G.K. and Oshlack, A. (2010) Gene ontology analysis for RNA-seq: accounting for selection bias. *Genome Biol.*, **11**, R14.
62. Kanehisa, M., Araki, M., Goto, S., Hattori, M., Hirakawa, M., Itoh, M., Katayama, T., Kawashima, S., Okuda, S., Tokimatsu, T. et al. (2008) KEGG for linking genomes to life and the environment. *Nucleic Acids Res.*, **36**, D480–D484.
63. Hughes, M.E., Hogenesch, J.B. and Kornacker, K. (2010) JTK_CYCLE: an efficient nonparametric algorithm for detecting rhythmic components in genome-scale data sets. *J. Biol. Rhythms*, **25**, 372–380.
64. De Donatis, G.M., Pape, E.L., Pierron, A., Cheli, Y., Hofman, V., Hofman, P., Allegra, M., Zahaf, K., Bahadoran, P., Rocchi, S. et al. (2016) NF- κ B2 induces senescence bypass in melanoma via a direct transcriptional activation of EZH2. *Oncogene*, **35**, 2735–2745.
65. Bhan, A., Hussain, I., Ansari, K.I., Bobzean, S.A., Perrotti, L.I. and Mandal, S.S. (2014) Histone methyltransferase EZH2 is transcriptionally induced by estradiol as well as estrogenic endocrine disruptors bisphenol-A and diethylstilbestrol. *J. Mol. Biol.*, **426**, 3426–3441.
66. Chen, H., Tu, S.W. and Hsieh, J.T. (2005) Down-regulation of human DAB2IP gene expression mediated by polycomb Ezh2 complex and histone deacetylase in prostate cancer. *J. Biol. Chem.*, **280**, 22437–22444.
67. Latimer, A.J., Shin, J. and Appel, B. (2005) her9 promotes floor plate development in zebrafish. *Dev. Dyn.*, **232**, 1098–1104.
68. Bae, Y.K., Shimizu, T. and Hibi, M. (2005) Patterning of proneuronal and inter-proneuronal domains by hairy- and enhancer of split-related genes in zebrafish neuroectoderm. *Development*, **132**, 1375–1385.
69. Martin, D.I., Zon, L.I., Mutter, G. and Orkin, S.H. (1990) Expression of an erythroid transcription factor in megakaryocytic and mast cell lineages. *Nature*, **344**, 444–447.
70. Romeo, P.H., Prandini, M.H., Joulín, V., Mignotte, V., Prenant, M., Vainchenker, W., Marguerie, G. and Uzan, G. (1990) Megakaryocytic and erythrocytic lineages share specific transcription factors. *Nature*, **344**, 447–449.
71. Long, Q., Meng, A., Wang, H., Jessen, J.R., Farrell, M.J. and Lin, S. (1997) GATA-1 expression pattern can be recapitulated in living transgenic zebrafish using GFP reporter gene. *Development*, **124**, 4105–4111.
72. Bennett, C.M., Kanki, J.P., Rhodes, J., Liu, T.X., Paw, B.H., Kieran, M.W., Langenau, D.M., Delahaye-Brown, A., Zon, L.I., Fleming, M.D. et al. (2001) Myelopoiesis in the zebrafish, *Danio rerio*. *Blood*, **98**, 643–651.
73. Quinkertz, A. and Campos-Ortega, J.A. (1999) A new beta-globin gene from the zebrafish, betaE1, and its pattern of transcription during embryogenesis. *Dev. Genes Evol.*, **209**, 126–131.
74. Lieschke, G.J., Oates, A.C., Crowhurst, M.O., Ward, A.C. and Layton, J.E. (2001) Morphologic and functional characterization of granulocytes and macrophages in embryonic and adult zebrafish. *Blood*, **98**, 3087–3096.
75. Herbomel, P., Thisse, B. and Thisse, C. (1999) Ontogeny and behaviour of early macrophages in the zebrafish embryo. *Development*, **126**, 3735–3745.
76. Kataoka, H., Ochi, M., Enomoto, K. and Yamaguchi, A. (2000) Cloning and embryonic expression patterns of the zebrafish Runt domain genes, runxa and runxb. *Mech. Dev.*, **98**, 139–143.
77. Thompson, M.A., Ransom, D.G., Pratt, S.J., MacLennan, H., Kieran, M.W., Detrich, H.W. 3rd, Vail, B., Huber, T.L., Paw, B., Brownlie, A.J. et al. (1998) The cloche and spadetail genes differentially affect hematopoiesis and vasculogenesis. *Dev. Biol.*, **197**, 248–269.
78. Willett, C.E., Kawasaki, H., Amemiya, C.T., Lin, S. and Steiner, L.A. (2001) Ikaros expression as a marker for lymphoid progenitors during zebrafish development. *Dev. Dyn.*, **222**, 694–698.
79. Langenau, D.M., Ferrando, A.A., Traver, D., Kutok, J.L., Hezel, J.P., Kanki, J.P., Zon, L.I., Look, A.T. and Trede, N.S. (2004) In vivo tracking of T cell development, ablation, and engraftment in transgenic zebrafish. *Proc. Natl. Acad. Sci. U.S.A.*, **101**, 7369–7374.
80. Willett, C.E., Zapata, A.G., Hopkins, N. and Steiner, L.A. (1997) Expression of zebrafish rag genes during early development identifies the thymus. *Dev. Biol.*, **182**, 331–341.
81. Choi, K., Kennedy, M., Kazarov, A., Papadimitriou, J.C. and Keller, G. (1998) A common precursor for hematopoietic and endothelial cells. *Development*, **125**, 725–732.
82. Liao, E.C., Paw, B.H., Oates, A.C., Pratt, S.J., Postlethwait, J.H. and Zon, L.I. (1998) SCL/Tal-1 transcription factor acts downstream of cloche to specify hematopoietic and vascular progenitors in zebrafish. *Genes Dev.*, **12**, 621–626.
83. Bracken, A.P., Pasini, D., Capra, M., Prosperini, E., Colli, E. and Helin, K. (2003) EZH2 is downstream of the pRB-E2F pathway, essential for proliferation and amplified in cancer. *EMBO J.*, **22**, 5323–5335.
84. Richter, G.H., Plehm, S., Fasan, A., Rossler, S., Unland, R., Bennani-Baiti, I.M., Hotfilder, M., Lowel, D., von Luettichau, I., Mossbrugger, I. et al. (2009) EZH2 is a mediator of EWS/FLI1 driven tumor growth and metastasis blocking endothelial and

- neuro-ectodermal differentiation. *Proc. Natl. Acad. Sci. U.S.A.*, **106**, 5324–5329.
85. Wilson, B.G., Wang, X., Shen, X., McKenna, E.S., Lemieux, M.E., Cho, Y.J., Koellhoffer, E.C., Pomeroy, S.L., Orkin, S.H. and Roberts, C.W. (2010) Epigenetic antagonism between polycomb and SWI/SNF complexes during oncogenic transformation. *Cancer Cell*, **18**, 316–328.
86. Doherty, C.J. and Kay, S.A. (2010) Circadian control of global gene expression patterns. *Annu. Rev. Genet.*, **44**, 419–444.
87. Zhang, R., Lahens, N.F., Ballance, H.I., Hughes, M.E. and Hogenesch, J.B. (2014) A circadian gene expression atlas in mammals: implications for biology and medicine. *Proc. Natl. Acad. Sci. U.S.A.*, **111**, 16219–16224.
88. Doi, M., Hirayama, J. and Sassone-Corsi, P. (2006) Circadian regulator CLOCK is a histone acetyltransferase. *Cell*, **125**, 497–508.
89. Tan, J.Z., Yan, Y., Wang, X.X., Jiang, Y. and Xu, H.E. (2014) EZH2: biology, disease, and structure-based drug discovery. *Acta Pharmacol. Sinica*, **35**, 161–174.
90. Mochizuki-Kashio, M., Mishima, Y., Miyagi, S., Negishi, M., Saraya, A., Konuma, T., Shinga, J., Koseki, H. and Iwama, A. (2011) Dependency on the polycomb gene Ezh2 distinguishes fetal from adult hematopoietic stem cells. *Blood*, **118**, 6553–6561.
91. Mendez-Ferrer, S., Lucas, D., Battista, M. and Frenette, P.S. (2008) Haematopoietic stem cell release is regulated by circadian oscillations. *Nature*, **452**, 442–447.
92. Nguyen, K.D., Fentress, S.J., Qiu, Y., Yun, K., Cox, J.S. and Chawla, A. (2013) Circadian gene Bmal1 regulates diurnal oscillations of Ly6C(hi) inflammatory monocytes. *Science*, **341**, 1483–1488.
93. Yan, J., Ng, S.B., Tay, J.L., Lin, B., Koh, T.L., Tan, J., Selvarajan, V., Liu, S.C., Bi, C., Wang, S. *et al.* (2013) EZH2 overexpression in natural killer/T-cell lymphoma confers growth advantage independently of histone methyltransferase activity. *Blood*, **121**, 4512–4520.